Mineralium Deposita (2005)
DOI 10.1007/s00126-005-0019-5

ARTICLE

Julie Hunt · Tim Baker · Derek Thorkelson

Regional-scale Proterozoic IOCG-mineralized breccia systems: examples from the Wernecke Mountains, Yukon, Canada

Received: 15 March 2004 / Accepted: 27 July 2005

Abstract A large scale Proterozoic breccia system consisting of numerous individual breccia bodies, collectively known as Wernecke Breccia, occurs in north-central Yukon Territory, Canada. Breccias cut Early Proterozoic Wernecke Supergroup sedimentary rocks and occur throughout the approximately 13 km thick deformed and weakly metamorphosed sequence. Iron oxide–copper–gold ± uranium ± cobalt mineralization is associated with the breccia bodies and occurs as veins and disseminations within breccia and surrounding rocks and locally forms the breccia matrix. Extensive sodic and potassic metasomatic alteration occurs within and around breccia bodies and is overprinted by pervasive calcite and dolomite/ankerite, and locally siderite, alteration, respectively. Multiple phases of brecciation, alteration and mineralization are evident. Breccia bodies are spatially associated with regional-scale faults and breccia emplacement made use of pre-existing crustal weaknesses and permeable zones. New evidence indicates the presence of metaevaporitic rocks in lower WSG that may be intimately related to breccia formation. No evidence of breccia-age magmatism has been found to date.

Keywords Wernecke Breccia · IOCG · Proterozoic · Iron oxide–copper–gold · Yukon

Editorial handling: I. McDonald

J. Hunt (✉)
Yukon Geological Survey, 300-345 Main Street,
Whitehorse, YT, Canada Y1A 2B5
E-mail: julie.hunt@gov.yk.ca
Tel.: +1-867-4563829
Fax: +1-867-3936232

J. Hunt · T. Baker
Economic Geology Research Unit, James Cook University,
Townsville, QLD 4811, Australia

D. Thorkelson
Simon Fraser University, Burnaby, BC, Canada

Introduction

Numerous Proterozoic breccia bodies, collectively known as Wernecke Breccia, occur over large areas in the north-central Yukon Territory of northern Canada (Fig. 1; cf. Bell 1986a, b; Thorkelson 2000). They are associated with extensive metasomatic alteration and potentially economically significant, but little studied, iron oxide–copper–gold ± uranium ± cobalt (IOCG) mineralization (cf. Bell and Delaney 1977; Bell 1978; Archer et al. 1977; Yukon MINFILE 2003) and represent some of the best preserved examples of Proterozoic-age IOCG mineralization in North America due to the relatively low grade of metamorphism. The scale of brecciation and alteration is similar to that in other large-scale Proterozoic breccia provinces including those in Australia that host the Ernest Henry (167 Mt at 1.1% Cu, 0.54 g/t Au; Ryan 1998) and giant Olympic Dam (> 600 Mt at 1.8% Cu, 0.5 kg/t U_3O_8, 0.5 g/t Au, 3.6 g/t Ag; Reynolds 2000) deposits. Several authors have drawn connections between the two areas based on similar ages and physical characteristics of the breccias and the possible proximity of ancestral North America to Australia in Proterozoic time (cf. Thorkelson et al. 2001a). However, unlike many IOCG districts where brecciation and mineralization are related to magmatism that acted as a source of fluid(s) (cf. Hitzman 2000; Sillitoe 2003), and/or provided heat to drive fluid circulation (cf. Barton and Johnson 1996, 2000) a clear relationship with magmatic rocks is not evident for Wernecke Breccias.

New mapping, petrographic and microprobe studies of several Wernecke Breccia-associated IOCG prospects have identified multiple brecciation, alteration and mineralizing events. In addition, the studies provide information on structural and stratigraphic features that control the location of breccia and associated alteration and mineralization and offer clues to the mechanism(s) of large-scale breccia formation.

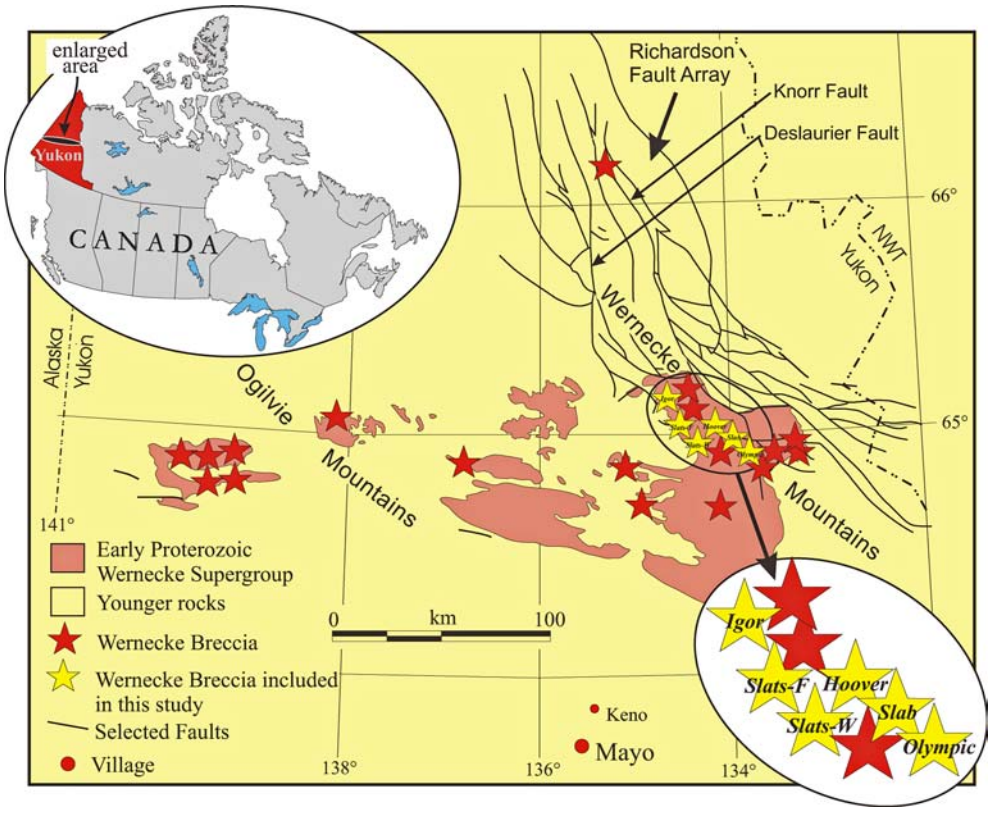

Fig. 1 Location of study area, distribution of WSG and Wernecke Breccia plus location of breccia-associated IOCG prospects included in this study (modified from Thorkelson, 2000)

Regional geologic setting

Wernecke Breccia bodies and associated IOCG mineralization occur in Early Proterozoic strata made up of Wernecke Supergroup (WSG), Bonnet Plume River Intrusions (BPRI), and "Slab volcanics[1]" (Figs. 2, 3; cf. Gabrielse 1967; Delaney 1981; Thorkelson 2000). The Early Proterozoic rocks are unconformably overlain by Middle Proterozoic Pinguicula Group carbonate and siliciclastic rocks (Fig. 3). The base of WSG is not exposed but is interpreted to sit on ≥1.84 Ga crystalline basement that is the westward continuation of the Canadian shield (cf. Norris 1997; Thorkelson 2000).

Wernecke supergroup

The Fairchild Lake, Quartet and Gillespie Lake groups make up the WSG and together form an approximately 13 km thick package of fine-grained marine sedimentary rocks and carbonates (Delaney 1981) that were deposited pre ca. 1,710 Ma as two clastic to carbonate grand cycles (cf. Thorkelson 2000). The Fairchild Lake Group (FLG) represents initial subsidence followed by infilling, and the Quartet and Gillespie Lake Groups (GLG) represent subsequent subsidence followed by infilling. The grand cycles may reflect continental rifting and equate to two stages of lithospheric stretching, subsidence and thermal deepening of the basin (Thorkelson 2000).

Fairchild lake group

The Fairchild Lake Group forms the basal part of the WSG and, in the study area, outcrops in a corridor which parallels the Bonnet Plume River valley (Fig. 2; Delaney 1981; Gordey and Makepeace 1999; Thorkelson 2000). It consists of at least 4 km of shallow marine sedimentary rocks that have been divided into five formations named, from base to top, F-1 to F-4 and F-Tr (Fig. 4; Table 1; Delaney 1981). Contacts between formations are conformable with the exception of F-4 which is considered to be facies equivalent to F-3; the contact between F-3 and F-Tr may, in part, be transitional (Delaney 1981). The formations are made up of variable amounts of grey-weathering, generally thin-bedded, commonly laminated, siltstone, mudstone, claystone and fine-grained sandstone; minor intercalated carbonate rocks occur in F-2 and F-Tr (*ibid.*).

Metaevaporites Previously unrecognised metaevaporites were identified in the Slab mountain area in strata that Bell and Delaney (1977) correlate with upper FLG. In general, evaporites dissolve during metamorphism and deformation, however they leave behind indirect evidence that they were once part of the stratigraphy (cf. Warren 1999). This evidence includes metamorphic

[1]Many of the names used in this paper are informal at present and are initially shown in quotation marks.

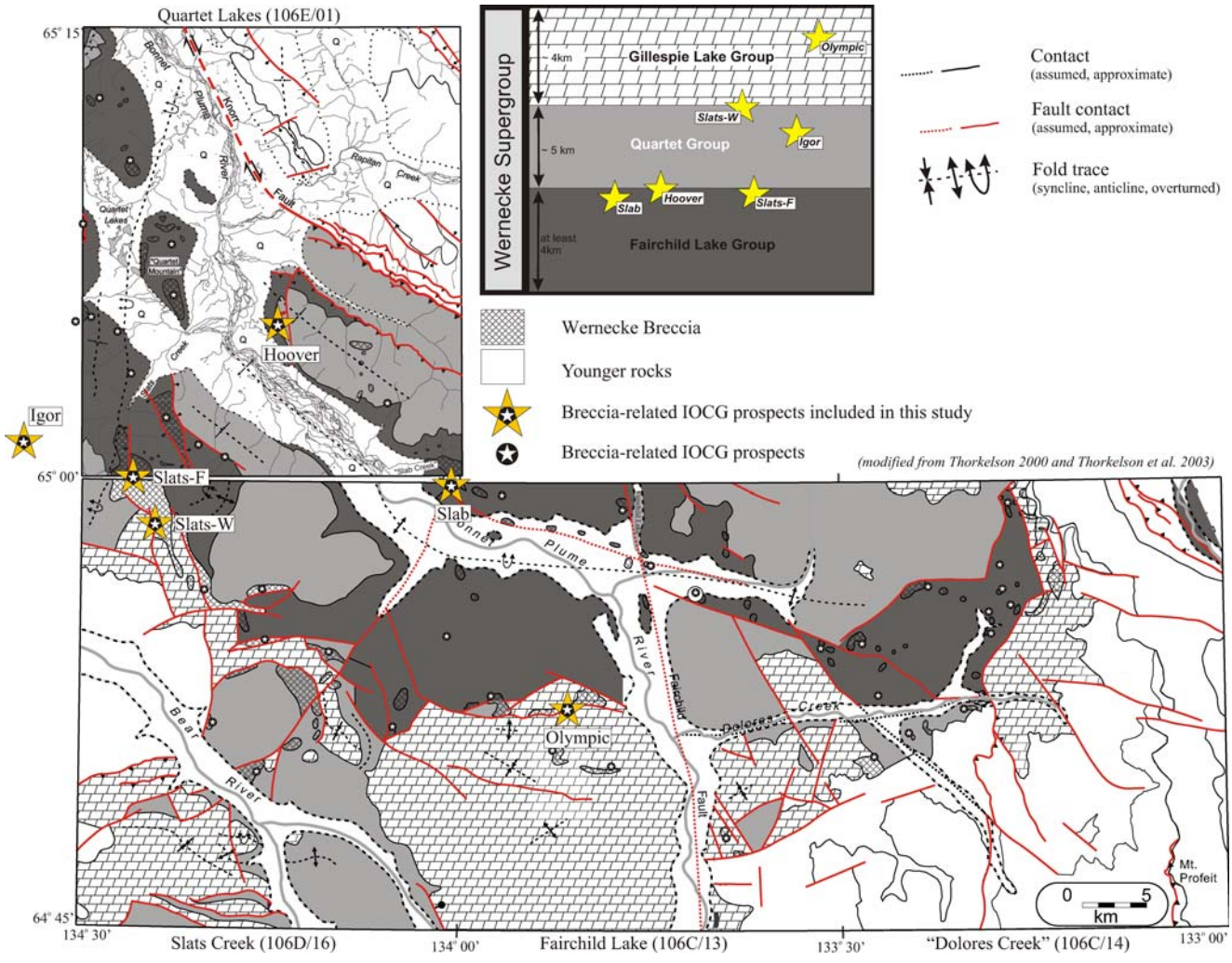

Fig. 2 Simplified geology map of the study area (for details see Thorkelson 2000; Thorkelson et al. 2002). Legend shows approximate stratigraphic position of IOCG prospects included in this study

minerals that are enriched in sodium (e.g. marialitic scapolite and albite) or magnesium (tourmaline and magnesium-rich biotite; cf. Kwak 1977; Warren 1999). The sodium comes from dissolution of salts such as halite and the magnesium from diagenetic minerals such as dolomite and clays (cf. Warren 1999). However, the presence of a likely metaevaporitic mineral assemblage does not, by itself, indicate an undeniable evaporite protolith because, for example, the NaCl in scapolite could have been derived from an outside source such as hydrothermal or sedimentary brines rather than halite. Further evidence is required from the distribution of the metaevaporitic mineral assemblage. Scapolites derived from hydrothermal or basinal brines tend to form haloes or replacement fronts associated with fluid conduits (Warren 1999). However, scapolite that is distributed as fine-scale interbedded scapolite-bearing and scapolite free layers is representative of an in situ salt precursor (*ibid.*). As evaporite dissolution occurs (during deposition, compaction, and/or during uplift associated with collision and basin inversion) strata overlying or intercalated with the evaporites settle and become fragmented leading to the formation of dissolution breccias. These breccias are commonly preserved in the rock record and are another indication of the former presence of evaporites (*ibid.*). Widespread sodic alteration haloes can also be an indication that evaporites were once part of the stratigraphy. The haloes form in fine-grained sediments adjacent to evaporites during burial, diagenesis and metamorphism due to progressive dissolution of evaporites by circulating fluids (*ibid.*). Resulting fluids are typically saline and chlorine-rich and lead to the growth of metamorphic minerals dominated by sodic phases, thus creating zones of albitisation or scapolitisation as scapolite replaces albite[2].

In the Slab area abundant (< 1 to 5 mm) scapolite occurs in discrete layers < 1 to 30 cm thick, in a sequence of fine-grained metasedimentary rocks at least 50 m thick (Figs. 4c, 5). The scapolite is sodium- and

[2] 3 Albite + NaCl ↔ Marialite i.e. 3 $Na(AlSi_3O_8)$ + NaCl ↔ $Na_4(Al_3Si_9O_{24})Cl$

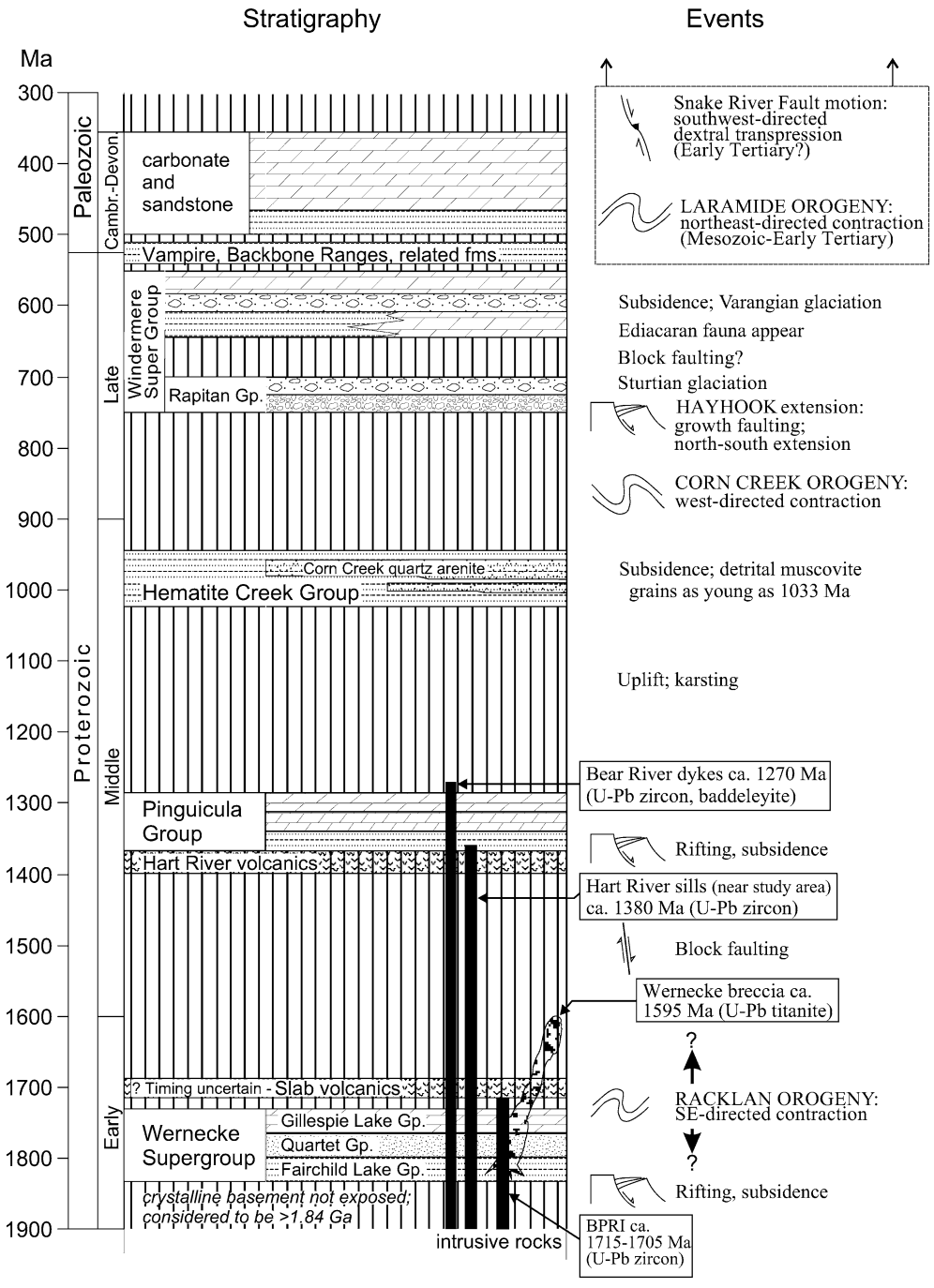

Fig. 3 Time stratigraphic column of the study area showing major depositional, intrusive and deformational events (modified from Thorkelson 2000)

chlorine-rich with a composition of 69.6–77.9% marialite ($Na_4[Al_3Si_9O_{24}]Cl$) and 22.1–30.4% meionite ($Ca_4[Al_6Si_6O_{24}]CO_3$); Na_2O content ranges from 7.94 to 10.24 wt.% (average 9.68 wt.%) and Cl content ranges from 2.90 to 3.55 wt. % (average 3.29 wt.%; Table 2). Biotite in this area is magnesium rich with MgO contents from 12.76 to 14.59 wt. % (average 13.75 wt. %; Table 2). The occurrence of scapolite within discrete layers and its marialitic composition are consistent with derivation from a protolith that contained abundant halite (cf. Warren 1999). The magnesium-rich nature of biotite associated with the scapolite is also consistent with this interpretation. Probable solution breccia made up of contorted, broken siltstone layers in a carbonate matrix occurs above the scapolite-rich horizon that underlies Slab ridge (Fig. 5). Large zones of sodic metasomatic alteration, typified by albite and marialitic scapolite, occur in fine-grained FLG sedimentary rocks in the Slab area consistent with expected alteration proximal to evaporite-bearing rocks. Taken together, the above indicate in situ (halite-facies) evaporites were once present in upper FLG strata.

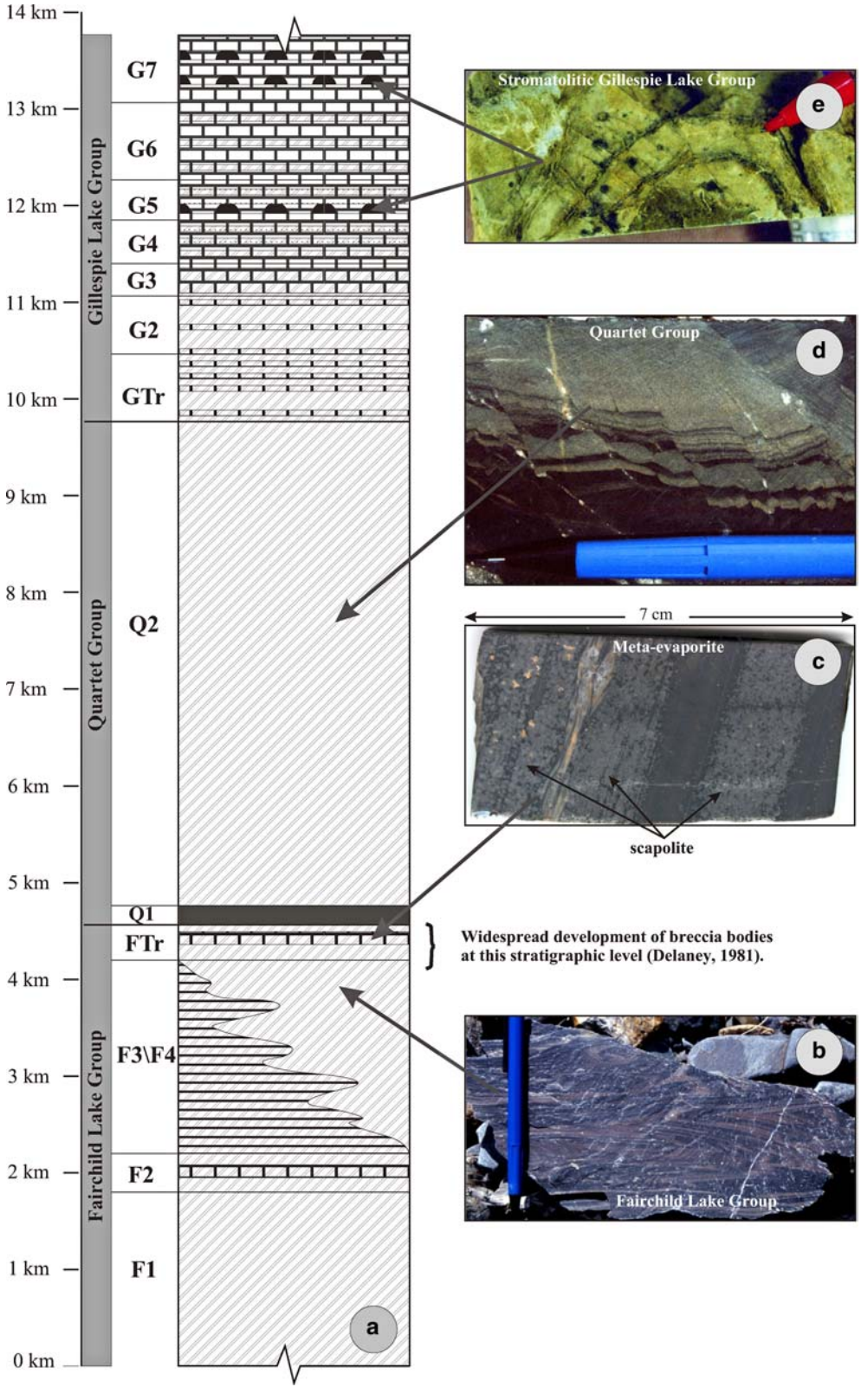

Fig. 4 WSG **a** stratigraphic column, see text and Table 1 for unit descriptions (information from Delaney 1981), **b** typical FLG, **c** probable meta-evaporite in F-Tr, **d** typical Quartet Group and **e** GLG stromatolitic dolostone

Quartet Group

The Quartet Group gradationally overlies the FLG and occurs throughout the study area (Fig. 2). It is at least 5 km thick and consists of a monotonous succession of dark grey-weathering clastic rocks that have been divided into basal black carbonaceous shale (Q-1) and conformably overlying, coarsening-upwards, interlay-

Table 1 Description of formations within WSG. Information from Delaney (1981)

Formation	Thickness (m)	Description	Sedimentary Structures
G-7	400 to 700	Thin to thick beds of orange-, buff-, and grey-weathering dolostone (patches of limestone); locally stromatolitic, locally carbonaceous. Lenses and nodules of grey chert.	Wavy and lenticular beds, parallel to crinkly laminations, oolites, pisolites, stromatolites, molar-tooth structure
G-6	500 to 800	Thin to thick beds of buff-, grey-, and maroon-weathering dolostone (locally carbonaceous), limestone, mudstone and siltstone.	Lenticular and wavy beds, parallel and cross laminations, load structures, microstylolites
G-5	$\sim$ 500	Thin to medium beds of buff-, grey, to locally maroon- or orange-weathering dolostone (locally carbonaceous) and claystone, minor siltstone and mudstone. Local thin to thick interbeds of stromatolitic dolostone conglomerate (granule- to pebble-sized clasts) and mounds, up to 3 m high, of brecciated stromatolitic dolostone (pebble- to cobble-sized clasts). Pods and lenses of dark grey chert.	Wavy and flaser beds, parallel and cross laminations, ripple marks, slump structures, stromatolites
G-4	$\sim$ 450	Thin beds of brown-, buff-, grey-, locally orange- or maroon-, recessive-weathering dolostone, mudstone and siltstone interlayered with up to 20% thin beds and lenses of grey chert.	Parallel to wavy laminations
G-3	At least 50	Medium to thick beds of buff-weathering silty dolostone.	Parallel laminations, tent structures
G-2	400 to 600	Brown-, grey- and orange-weathering mudstone and lesser siltstone and silty dolostone. Minor lenses of black chert.	Laminations, lenticular beds, load structures
G-Tr	25 to 700	Grey-weathering siltstone, fine-grained sandstone and mudstone interlayered with thin beds of orange- to brown-weathering silty dolostone and dolomitic siltstone.	Parallel- and cross-laminations, wavy, lenticular and flaser-bedding, graded bedding, ripple marks, load structures, flame structures, shrinkage cracks, slump folds
Q-2	$\leq$ 5000	Thin-, medium- to thick-bedded grey-weathering siltstone, mudstone, fine-grained sandstone and claystone.	Parallel- and cross-laminations, wavy, lenticular and flaser-bedding, graded bedding, ripple marks, load structures, flame structures, shrinkage cracks, slump folds
Q-1	$\sim$ 200	Dark grey-weathering, thin-bedded, locally pyritic, carbonaceous claystone, clayey siltstone and carbonaceous mudstone.	None – sediments have generally been metamorphosed to slate
F-Tr	$\leq$ 365	Grey-, brown- to white-weathering slate, mudstone, siltstone, dolomitic mudstone, silty dolostone and limestone. 7–14 m-thick limestone marker.	Cross-beds, molar tooth structures
F-4	$>$ 500	Thin to thick beds of grey-weathering siltstone, fine-grained sandstone and mudstone.	Parallel- to cross-laminations to wavy beds, ripple marks, cross-beds
F-3	$\sim$2000	Thin to medium beds of grey-weathering siltstone, mudstone and fine-grained sandstone, minor intercalated thin beds of silty limestone.	Parallel laminations to lenticular beds, ripple marks, load structures, flutes
F-2	$\sim$400	Thin-bedded grey to buff-weathering siltstone, mudstone, fine-grained sandstone and silty to sandy limestone.	Wavy to planar to lenticular beds/laminations, cross-beds, load structures
F-1	$>$ 1800	Thin to medium beds of grey-weathering siltstone, mudstone and fine-grained sandstone, minor limestone.	Laminated to lenticular beds, asymmetrical cross-beds, ripple marks, load structures

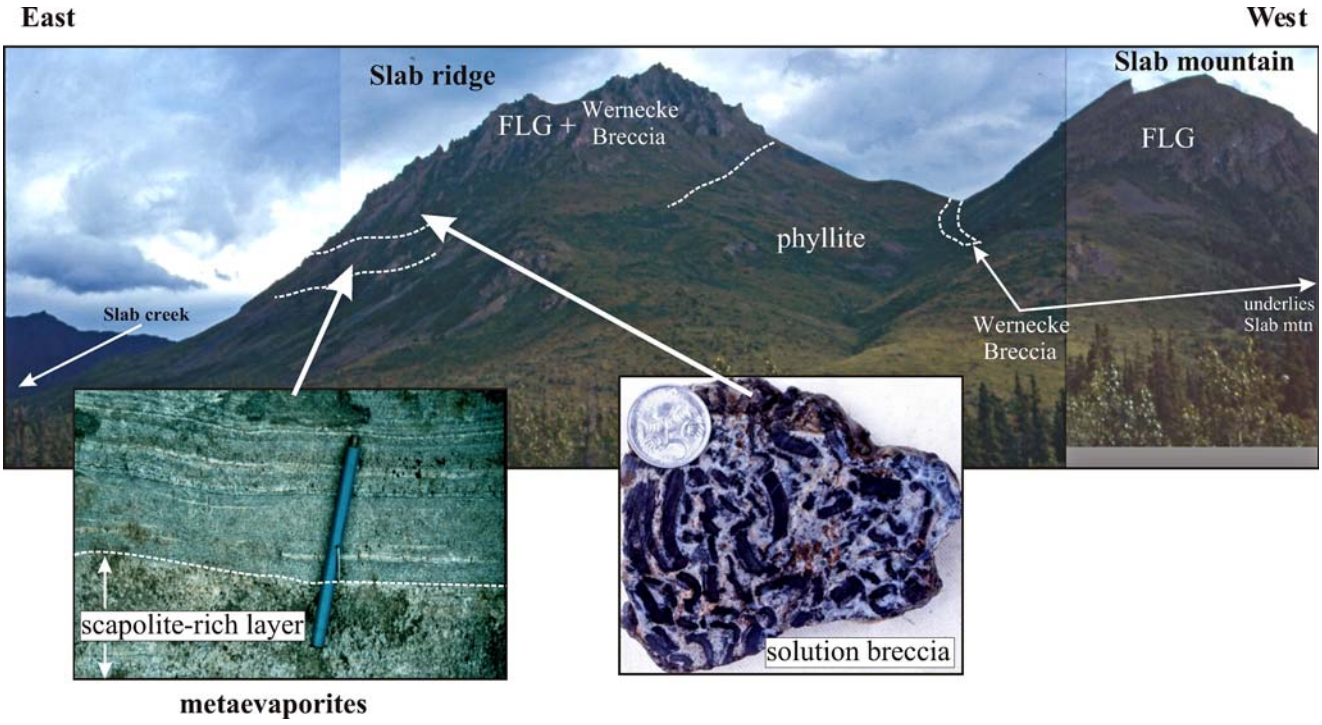

Fig. 5 View of Slab mountain and Slab ridge (*looking south*) showing location of metaevaporites. Insets: detail of metaevaporites in outcrop showing one thick (*labelled*) and several narrow (*light coloured*) scapolite-rich layers and detail of solution breccia that overlies metaevaporites

ered, shale, siltstone and sandstone (Q-2; Fig. 4a, d; Table 1; Delaney 1978, 1981). Q-1 is interpreted to have accumulated in a sediment-starved basin (Delaney 1981). Q-2 was deposited in a shallow marine (subtidal to intertidal) environment and records a gradually increasing influx of sediment into the basin (*ibid.*).

Gillespie Lake Group

The Gillespie Lake Group gradationally overlies the Quartet Group and forms the upper part of the WSG. It occurs throughout the study area (Fig. 2) and consists of at least 4 km of shallow marine, buff-, orange- and locally grey-weathering dolostone, limestone, claystone, mudstone, and sandstone divided into seven conformable formations named, from base to top, G-Tr and G-2 to G-7 (Fig. 4a; Table 1; Delaney 1978, 1981). G-Tr consists of siliciclastic sediments that gradually increase in carbonate content up sequence (Delaney 1981). G-2 to G-4 are made up of fine-grained siliciclastic-dolostone admixtures. G-5 is similar to G-2 to G-4 but contains stromatolitic conglomerate and brec-

Table 2 Representative results of scapolite and biotite microprobe analyses. % meionite = 100 (Ca + Mg + Fe + Mn + Ti)/(Na + K + Ca + Mg + Fe + Mn + Ti); marialite = 100 - meionite (after Deer et al. 1992)

Oxide (weight %)	Scapolite Min - Max	Scapolite [a] Average	Biotite Min – Max	Biotite[b] Average
SiO_2	54.61–57.73	56.08	37.27–40.64	38.92
TiO_2	0.00–0.04	0.01	1.33–2.57	2.00
Al_2O_3	21.12–22.54	21.78	14.79–13.23	14.00
FeO	0.00–0.09	0.04	12.97–15.53	14.28
MnO	0.00–0.04	0.01	0.04–0.43	0.19
MgO	0.00–0.01	0.00	12.76–14.59	13.75
CaO	5.34–7.13	6.34	0.00–0.37	0.17
Na_2O	7.94–10.24	9.68	0.00–0.61	0.08
K_2O	0.44–1.21	0.55	9.96–10.63	10.27
Cl	2.90–3.55	3.29	0.46–0.72	0.59
Total	96.09–98.97	97.77	91.21–97.49	94.25
% Meionite $Ca_4[Al_6Si_6O_{24}]CO_3$	22.12–30.44	25.98		
% Marialite $Na_4[Al_3Si_9O_{24}]Cl$	69.56–77.88	74.02		

Analyses were obtained with the James Cook University JEOL electron microprobe in wavelength dispersive mode, at an accelerating voltage of 15 kV and a current of 20 nA, ZAF corrections were used

[a] Average of 70 analyses

[b] Average of ten analyses

Table 3 Main characteristics of IOCG prospects included in this study, see text for details

Prospect	Resource/best intersection	Metals	Mineralization (dominant)	Alteration (dominant)	Stratigraphic setting	Structural setting
Slab (106D 070)[a]	20 million tons of 0.35% Cu & 0.17 gpt Au[b]	Fe, Cu, Au ± Mo, Co, U	Magnetite^{VD}, hematite^{VDB} chalcopyrite^{VDB}, pyrite^{VDB} ± brannerite^{VD}, molybdenite^{D}, cobaltite^{D}	Pervasive albite-scapolite ± orthoclase; calcite veins	Upper FLG interlayered fine-grained calcareous metasedimentary rocks & minor carbonate; halite-facies metaevaporites	Folds, high strain zone(s), permeable strata
Hoover (106E 002)[a]	0.32 gpt Au & 0.42% Cu over 73 m[b]; 3.6% Cu over 3.1 m[b,c]	Fe, Cu, Au ± U, Co	Magnetite^{VD}, hematite^{VDB}, pyrite^{VDB}, chalcopyrite^{VDB} ± brannerite^{VD}	Pervasive albite ± scapolite; calcite ± dolomite veins	Transition from FLG fine-grained calcareous metasedimentary rocks to Quartet Group carbonaceous shale/slate	Folds, high strain zone
Slats-F (106D 075)[a]	1380 ppb Au & 9650 ppm Cu from a grab sample[b]	Fe, Cu, Au ± Co	Magnetite^{VD}, hematite^{VDB}, minor chalcopyrite^{VD}, pyrite^{VD}	Pervasive orthoclase; dolomite-ankerite veins	?FLG fine-grained calcareous metasedimentary rocks	Fold, high strain zone, fractures, pathways previously used by BPRI, permeable strata
Slats-W (106D 075)[a]	450 ppb Au, 1115 ppm Cu, 5800 ppm Co over 1 m[d]	Fe, Cu ± Co, U, Au	Magnetite^{VD}, pyrite^{VDB}, hematite^{VDB}, chalcopyrite^{VD} ± cobaltite^{D}, brannerite^{VD}	Pervasive orthoclase; dolomite-ankerite veins	Interlayered shale and fine-grained calcareous metasedimentary rocks at the transition from Quartet Group to GLG	pathways previously used by BPRI, permeable strata
Igor (106E 009)[a]	4.74% Cu, 0.088% U_3O_8, 325 ppm Co over 19.7 m[e]; 6.14% Cu, 0.89% U_3O_8 and 358 ppm Co over 10.6 m[e]	Fe, Cu, U ± Co, Au	Magnetite^{VDB}, hematite^{VDB}, pyrite (some is cobaltian)^{VDB}, chalcopyrite^{VDB}, barite^{VD} ± pitchblende^{VD}	Pervasive orthoclase-sericite ± albite; dolomite- ankerite-siderite veins; disseminated siderite; disseminated and vein barite	Quartet Group fine-grained calcareous metasedimentary rocks with well preserved sedimentary structures, e.g. ripple marks	Fold, high strain zone
Olympic (106C 095)[a]	1593 ppm Cu, 40 ppm Co & 23 ppb Au over 11 m[f]; 0.8% Cu, 14 ppm Co over 1.7 m[f]	Fe, Cu ± Co, Au	Hematite^{VDB}, pyrite^{VD}, chalcopyrite^{VD} ± cobaltite^{D}	Pervasive and vein dolomite-ankerite; locally pervasive orthoclase;	GLG dolostone (locally stromatolitic)	Folds, faults, pathways previously used by BPRI

In mineralization column: *V* vein, *D* disseminated, *B* forms breccia matrix

[a]Yukon MINFILE (2003) database number. Information from: [b](Thorkelson et al. 2003), [c](Yukon MINFILE 2003), [d](Stammers 1995), [e] (Eaton and Archer 1981) and [f](Caulfield 1994)

cia. G-6 is made up of thick sequences of carbonate and terrigenous-carbonate admixtures. G-7 consists of platformal carbonates some of which are stromatolitic (Fig. 4e).

Igneous rocks

Numerous small Early Proterozoic (ca. 1,715 to 1,705 Ma) igneous bodies, known as Bonnet Plume

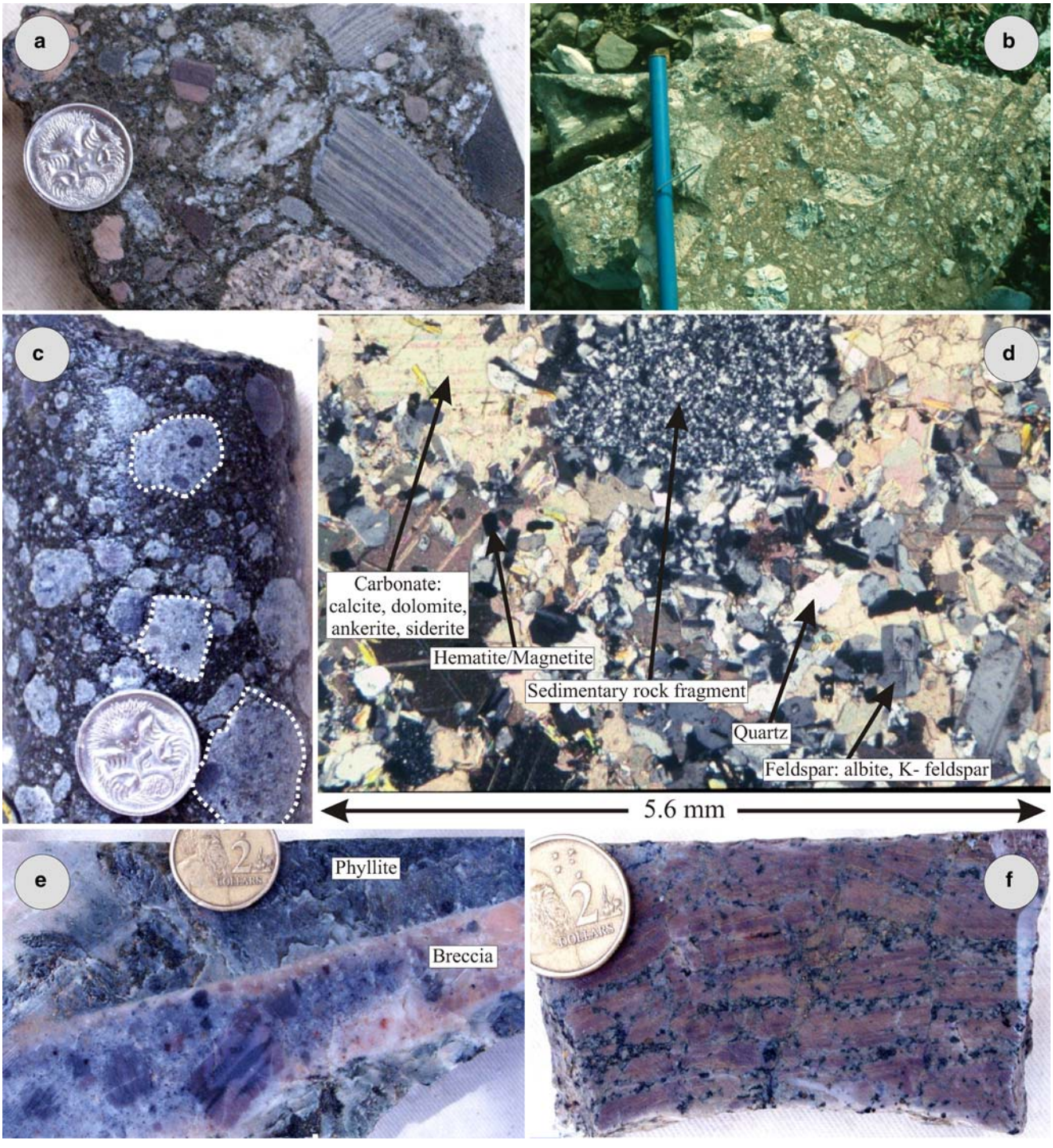

Fig. 6 Examples of Wernecke Breccia: **a** clast supported breccia, Slab area, **b** matrix supported breccia, Olympic area, **c** breccia with abundant clasts of earlier breccia, Slab area, **d** photomicrograph of Wernecke Breccia matrix (*crossed polars*) made up dominantly of sedimentary rock fragments, carbonate, feldspar, lesser quartz and minor hematite and magnetite, **e** sharp contact between breccia and phyllitic metasiltstone, Hoover area, **f** crackle brecciated metasiltstone from a gradational breccia contact, Hoover area

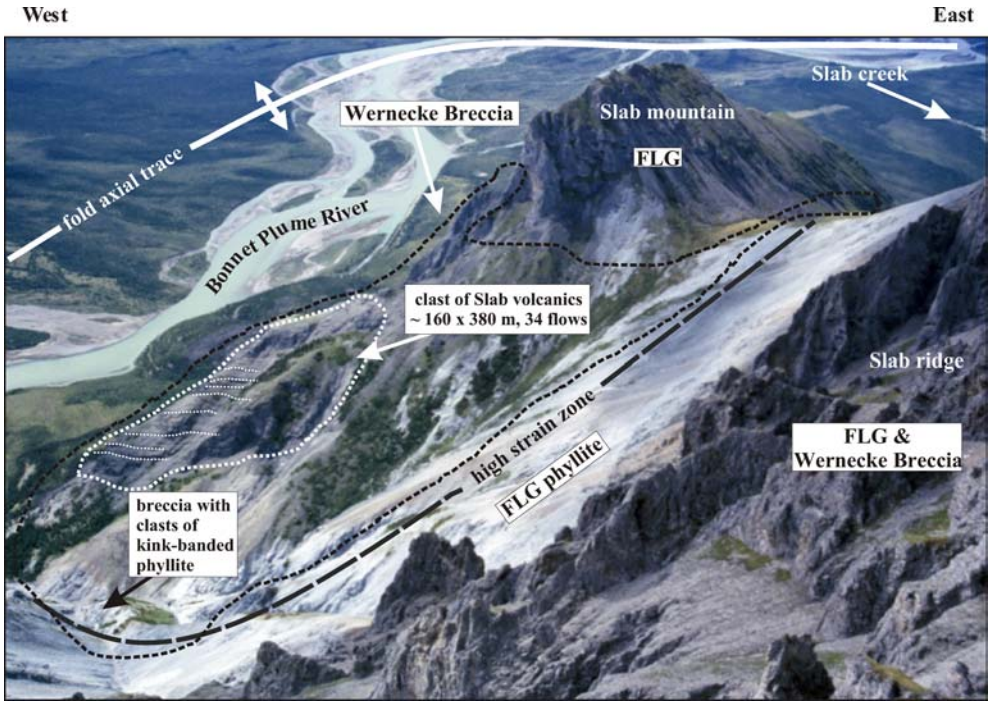

Fig. 7 Slab mountain area showing location of 'Slab mountain', 'Slab ridge', 'Slab creek', Bonnet Plume River, fold axial trace in the river valley, Wernecke Breccia, high strain zone, breccia that contains deformed clasts of phyllite and large clast of Slab volcanics with some of the flows outlined

River Intrusions (BPRI), crosscut the WSG and occur as clasts in Wernecke Breccia (Fig. 3; Thorkelson 2000; Thorkelson et al. 2001a, 2001b). The intrusions are generally fine- to medium-grained and composed of rift-related tholeiitic diorite or gabbro and lesser syenite and anorthosite (Thorkelson et al. 2001b).

Slab volcanics are preserved as clasts within Wernecke Breccia (cf. Thorkelson 2000). The main exposure is a 160×380 m block comprising about 34 steeply dipping, 0.8 to 14 m thick, mafic to intermediate, subaerial flows and minor intercalated volcaniclastic and epiclastic units (cf. Laughton et al. 2002; Laughton 2004). The age of the volcanic rocks is not known. They are geochemically similar to BPRI and may have been comagmatic with them, thus Slab volcanics could be younger than WSG (cf. Thorkelson 2000). Alternatively, Slab volcanics may be part of lower WSG. They have only been observed in Wernecke Breccia emplaced into upper FLG strata in several localities along the Bonnet Plume River valley (Thorkelson 2000; Laughton et al. 2002; Laugh-

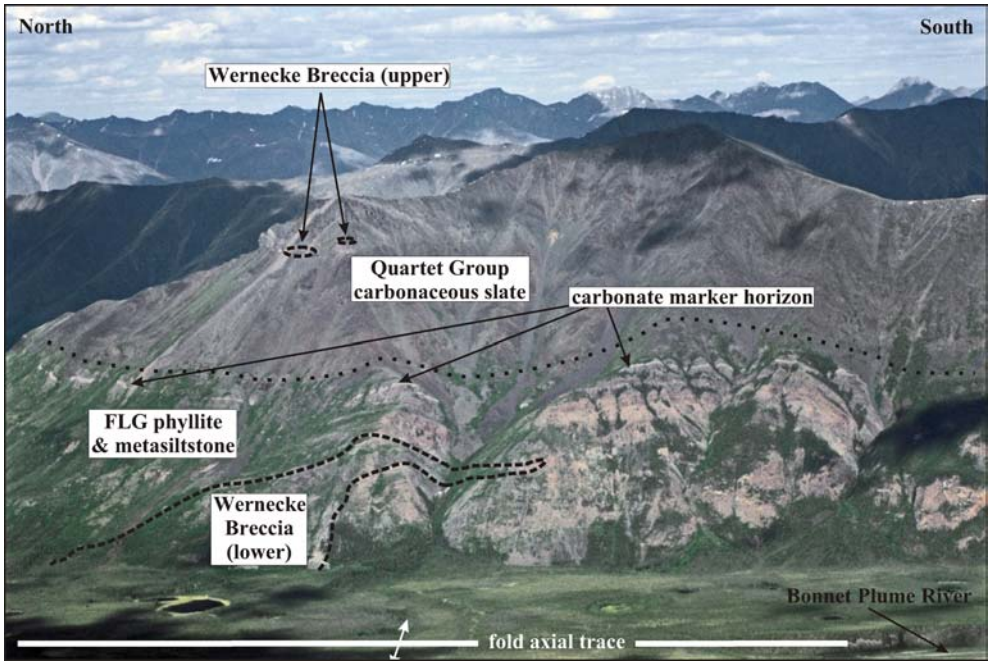

Fig. 8 Hoover area showing location of FLG, Quartet Group, marker carbonate horizon and upper and lower breccias. (Photo taken by D.J. Thorkelson)

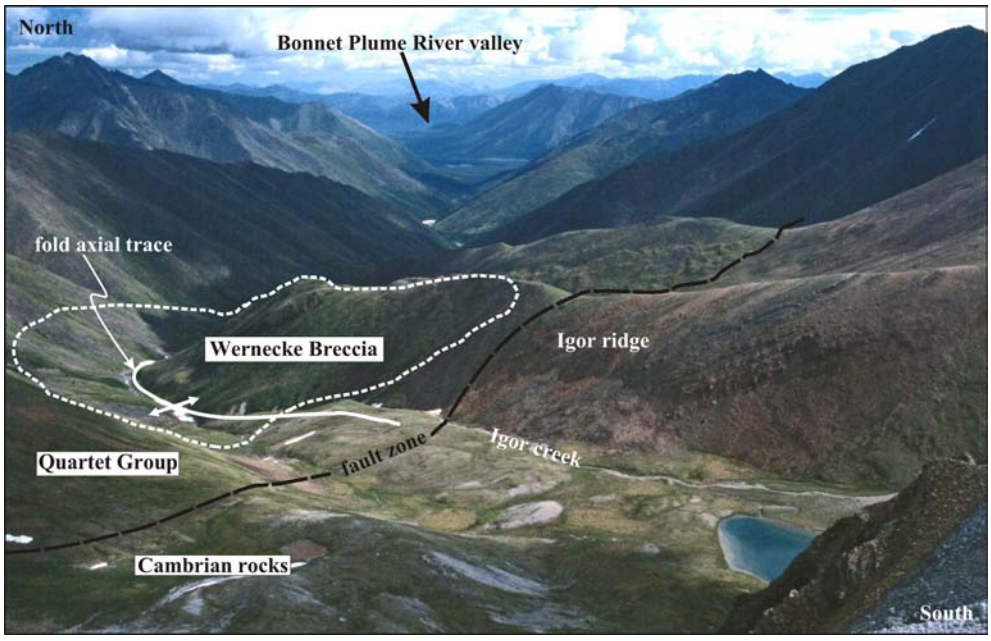

Fig. 9 Igor area showing location of 'Igor ridge', fold axial trace in 'Igor creek', Wernecke Breccia, Quartet Group and Cambrian strata

ton 2004; this study). Clasts within Wernecke Breccia appear to be locally derived from proximal host rocks (WSG or BPRI), thus it seems reasonable to assume clasts of Slab volcanics were also locally derived. Therefore, the eruption of Slab volcanics may have been a localized event during lower WSG deposition. The WSG is a dominantly marine succession and Slab volcanics are subaerial however, the presence of meta-evaporites within lower WSG rocks indicates very shallow marine to emergent conditions were present at least periodically, thus sub-aerial volcanism could have occurred during deposition of lower WSG strata.

Metamorphism, deformation, and timing

The Racklan Orogeny produced lower to middle greenschist grade regional metamorphism in WSG rocks (cf. Delaney 1981; Thorkelson 2000, Brideau et al. 2002). Typical metamorphic mineral assemblages include chlorite–muscovite–chloritoid–quartz ± garnet indicating peak metamorphic conditions of 450–550°C and approximate pressure of 3–6 kbars (Brideau et al. 2002). Three phases of deformation are ascribed to the Racklan Orogeny (Thorkelson 2000; Brideau et al. 2002). The first phase occurred during peak metamorphism and produced foliations (ranging from slaty cleavage to schistosity) and north- to east-trending folds (*ibid.*). The second phase produced crenulations and local crenulation cleavage and the third phase led to the formation of kink-bands. During Racklan orogenesis some units, especially those in the upper FLG and Quartet Group, were converted to schist, slate and phyllite in regions of high strain, commonly in the cores, or overturned parts, of tight folds (cf. Thorkelson et al. 2003). The age of the Racklan Orogeny is not known however it is constrained by the age of Wernecke Breccia that contains clasts of deformed WSG (Fig. 3). In the Slab area, hydrothermal titanite from the matrix of Wernecke Breccia that contains clasts of foliated, kinked metasiltstone returned a U-Pb age of ca. 1,600 Ma (Thorkelson et al. 2001a), thus, the Racklan Orogeny must be older than ca. 1,600 Ma.

Cross-cutting relationships indicate both the BPRI and the Slab volcanics are older than Wernecke Breccia, i.e. the breccia contains clasts of these lithologies (Thorkelson 2000). The difference in age between the igneous rocks and the breccia is poorly constrained due to the unknown age of the Slab volcanics and minimal reliable age information for Wernecke Breccia. However, available data for the breccias indicate they are significantly younger than BPRI, i.e. ca. 1,600 Ma versus ca. 1,710 Ma (Thorkelson 2000; Thorkelson et al. 2001a, 2001b). The timing of magmatism relative to Racklan deformation remains uncertain as there are no documented outcrops of BPRI or Slab volcanics that contain Racklan deformation fabrics (*ibid.*). Both the BPRI and the Slab volcanics have been affected by low grade metamorphism—for example in the BPRI, pyroxene has altered to chlorite or actinolite and plagioclase is replaced by sericite, albite, potassium feldspar or scapolite (Thorkelson et al. 2001b) and in the Slab volcanics plagioclase is commonly replaced by scapolite (Thorkelson 2000; Laughton et al. 2002; Laughton 2004). However, some (or all) of this alteration may be due to metasomatism associated with Wernecke Breccia emplacement.

Several post-Racklan orogenic events also affected the study area (Fig. 3). The Middle Proterozoic Corn Creek Orogeny produced west- to southwest-verging folds and thrust faults mainly in the Pinguicula and

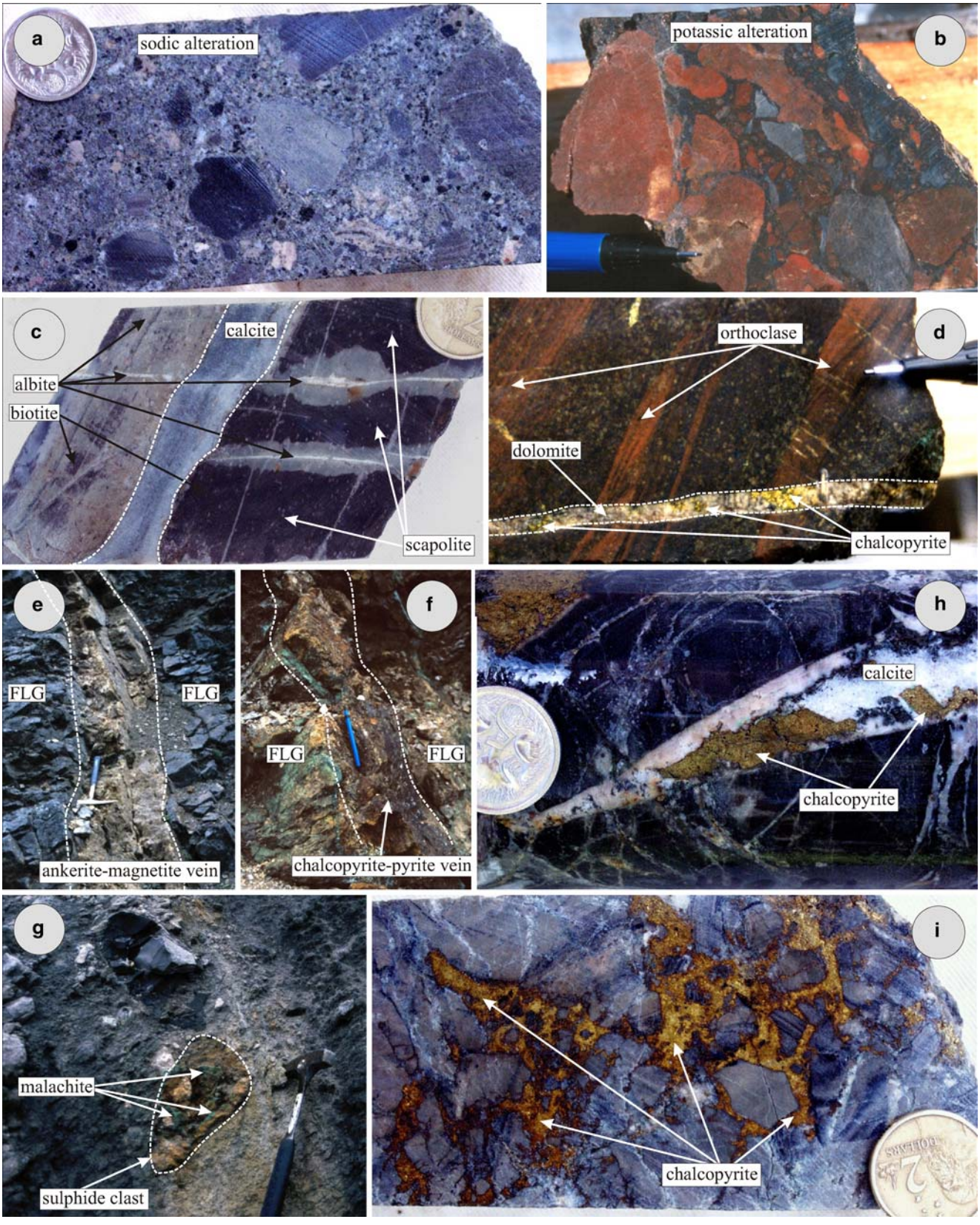

Fig. 10 Examples of alteration and mineralization: **a** grey sodic-altered breccia, **b** red potassic-altered breccia, **c** biotite–scapolite alteration in FLG metasiltstone cut by albite veins, cross-cut by calcite vein, **d** potassic-altered Quartet Group metasiltstone cut by dolomite-chalcopyrite vein, **e** ankerite-magnetite vein cutting FLG, Slab prospect, **f** massive chalcopyrite-pyrite vein cutting FLG, Slab prospect, **g** clast of massive sulphide in breccia, Slab prospect, **h** calcite-chalcopyrite vein cutting FLG, Slab prospect and **i** chalcopyrite forming matrix to breccia, Hoover prospect

Hematite Creek groups (Fig. 3; Thorkelson 2000). The Late Proterozoic Hayhook extensional event produced generally west-trending normal faults some of which truncate folds and faults related to the Corn Creek Orogeny (*ibid.*). Contractional deformation associated with the Cretaceous to Early Tertiary Laramide Orogeny produced large-wavelength, west–northwest-trending folds and reverse faults in WSG and younger strata (Fig. 2; Norris 1997; Thorkelson et al. 2003). Laramide-age structures are cut by Tertiary normal faults (Thorkelson 2000).

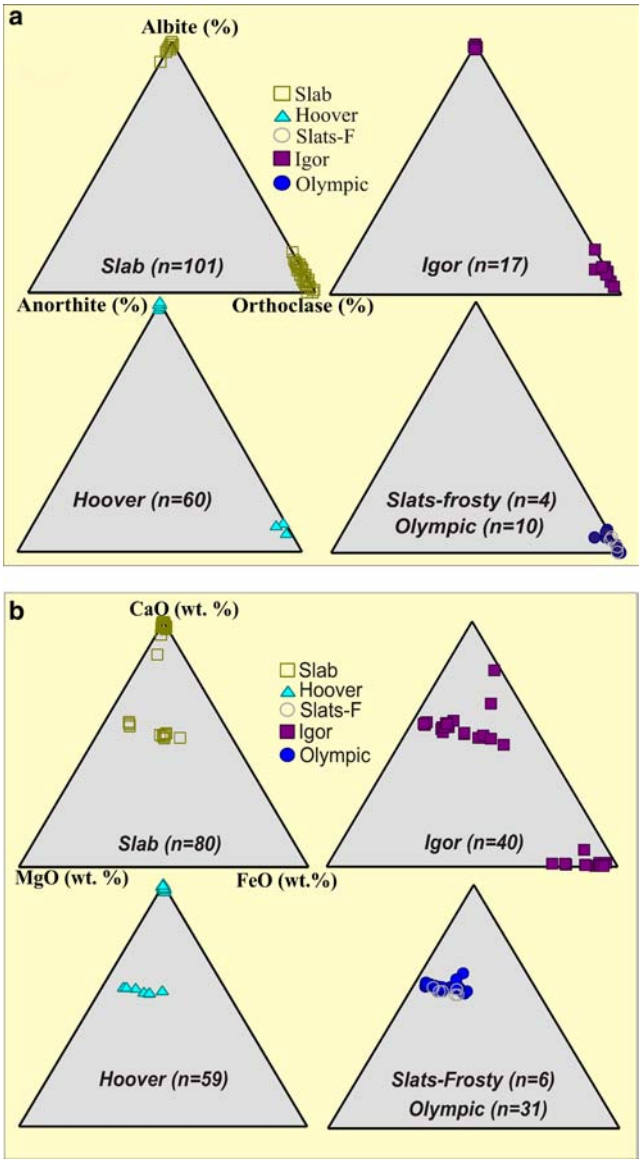

Fig. 11 Composition of **a** feldspar and **b** carbonate in Wernecke samples, based on microprobe data. Analyses were obtained with the James Cook University electron microprobe in wavelength dispersive mode, at an accelerating voltage of 15 kV and a current of 20 nA

Geology of Wernecke Breccia

Six widely spaced IOCG prospects were examined in this study (Figs. 1, 2): Slab, Hoover, Igor, Slats-Frosty, Slats-Wallbanger and Olympic. The prospects were chosen based on: differences in metasomatic alteration [M. Stammers personnel communications 2000; R. Gorton pers comm. 2000]; stratigraphic location within host WSG strata (Eaton and Archer 1981; Thorkelson 2000); and the availability of diamond drill core. Mapping was carried out at 1:5,000 scale at Slab, Hoover and Igor (Hunt et al. 2002; Thorkelson et al. 2002, 2003); reconnaissance mapping was carried out at the remaining prospects. Diamond drill core from each of the prospects was logged in detail[3] and samples collected for petrographic, microprobe, stable isotope and fluid inclusion analyses. Mapping and core logging were carried out in order to characterize the structural and stratigraphic settings of the breccias and associated alteration and mineralization, and to provide paragenetic information. This paper presents the results of field, petrographic and microprobe studies. Stable isotope and fluid inclusion data will be presented in detail in a later paper (Hunt et al. in preparation); a summary is given here. The main characteristics of the prospects are summarized in Table 3 and described below beginning with a general description of Wernecke Breccia based on combined observations from the prospects studied.

Wernecke Breccia varies from clast to matrix supported (Fig. 6a, b; cf. Bell 1986a, b; Thorkelson 2000; Hunt et al. 2002). Clasts are generally sub-angular to sub-rounded and range from $<$ 1 cm to metres to several hundred metres across (e.g. Slab Fig. 7). Clasts are locally derived, dominantly from proximal WSG strata, however, clasts of BPRI (e.g. at Slab, Hoover, Olympic) and Slab volcanics (e.g. at Slab) are abundant where breccia cuts those lithologies. Early phases of Wernecke Breccia are preserved in some locations as clasts within later breccia (Fig. 6c). Breccia matrix is made up of rock fragments and hydrothermal precipitates consisting mainly of feldspar (albite and/or potassium feldspar), carbonate (calcite, or dolomite/ankerite, locally siderite) and quartz (Fig. 6d). Locally, the breccia matrix contains abundant hematite, magnetite, chalcopyrite (see Mineralization section), biotite, muscovite barite and fluorite and lesser tourmaline and actinolite, and rare titanite and monazite. In some places, the matrix is coarsely crystalline and is made up of quartz, calcite and fluorite crystals up to 2 cm across. Locally, biotite, muscovite and magnetite crystals up to 1 cm across occur within finer grained matrix.

[3]The following number of diamond drill holes were logged in detail at Slab, Hoover, Slats-Frosty, Slats-Wallbanger, Igor and Olympic respectively: 5, 2, 2, 3, 2 and 3. An additional eight holes were examined in less detail at Slab.

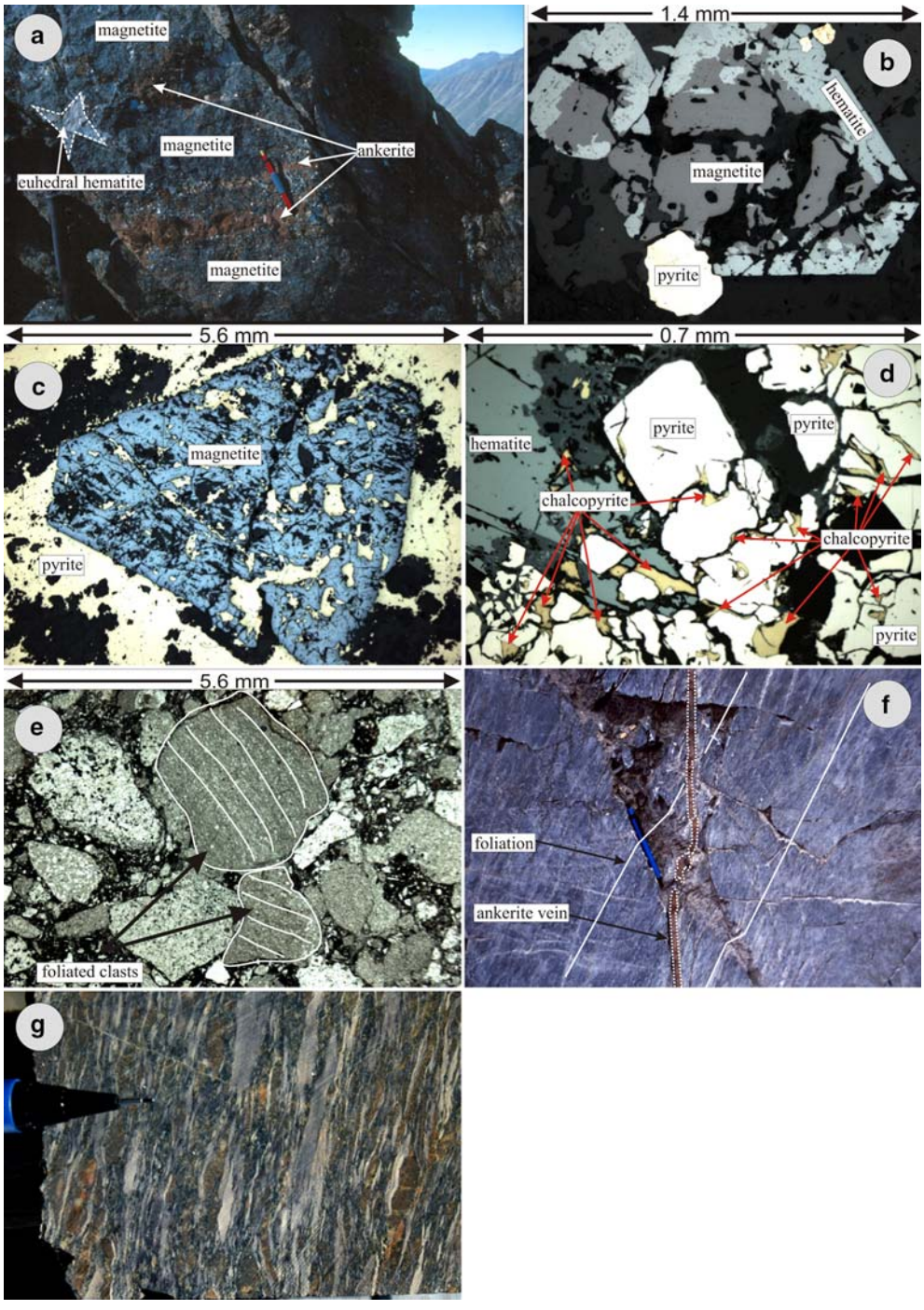

Fig. 12 Examples of mineralization and deformation: **a** massive magnetite-coarsely crystalline hematite-ankerite-quartz vein, Slats-Frosty area, **b** euhedral magnetite replaced by hematite (rl), Igor prospect, **c** euhedral magnetite overgrown by pyrite (rl), Igor prospect, **d** hematite overgrown by pyrite with chalcopyrite filling fractures (rl), Olympic prospect, **e** clasts of foliated metasiltstone in Wernecke Breccia, **f** foliated FLG cut by ankerite vein, both have been kinked during Racklan deformation and **g** flattened clasts in foliated breccia. *rl* reflected light

Wernecke Breccia complexes vary greatly in shape and size. In plan view, they are elliptical, elongate, or irregular in shape. In vertical section, they can be discordant or parallel to layering with no or numerous offshoots. The size of breccia bodies varies from a few centimetres to several hundred metres to several kilometres across. Contacts between country rock and breccia vary from sharp to diffuse/gradational (Fig. 6e, f). Gradational boundaries with the WSG extend for a few centimetres to several tens of metres and the degree of brecciation gradually decreases outwards from strongly disrupted sedimentary rocks to layers that appear simply ''pushed apart'' to fractured country rock.

Wernecke Breccia: structural and stratigraphic controls

Regional scale

Wernecke Breccias are spatially associated with regional-scale faults (cf. Bell 1986a, b; Thorkelson 2000). In the study area, breccia bodies lie on the southwestern

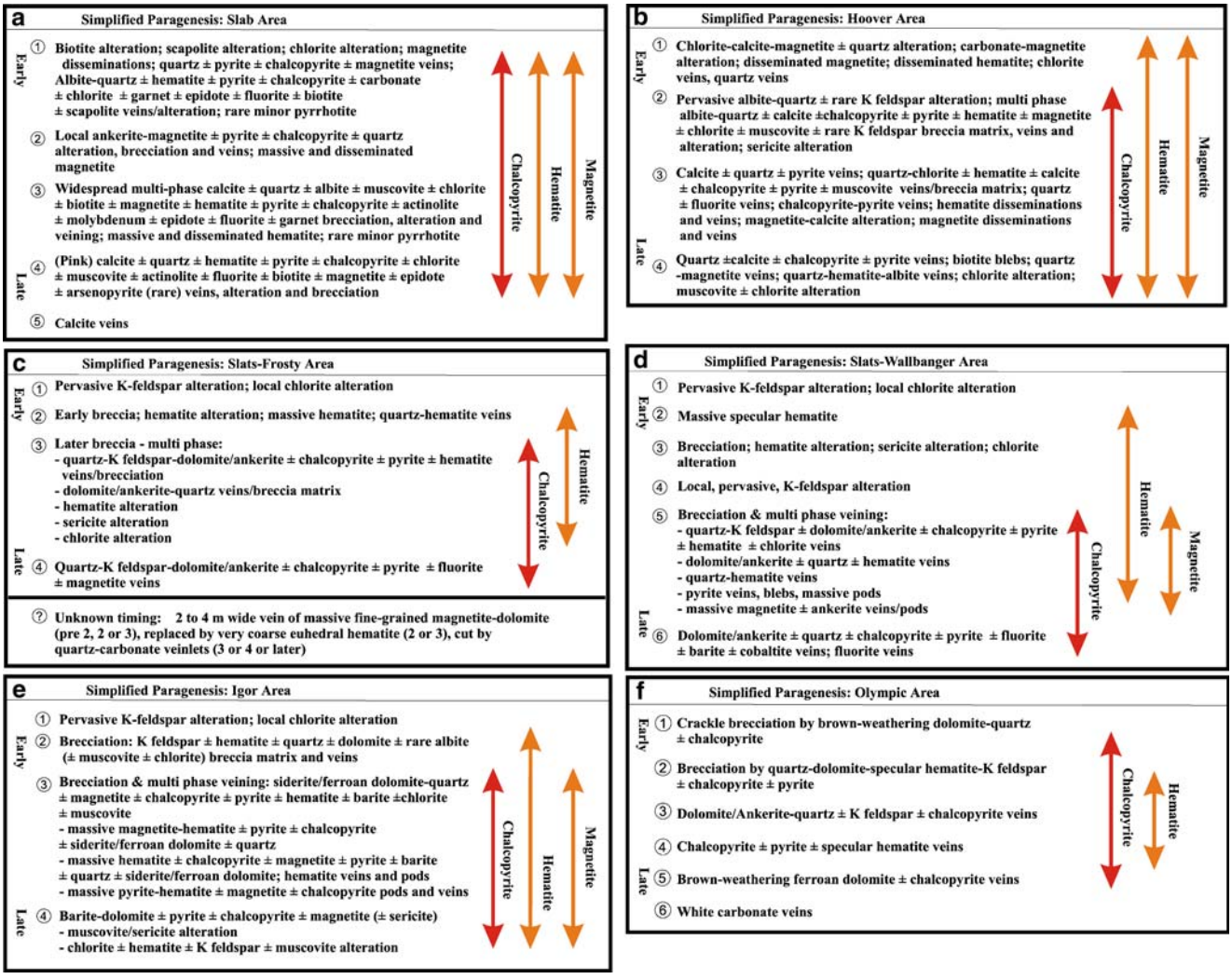

Fig. 13 Simplified paragenesis for prospects in the Wernecke Mountains : **a** Slab, **b** Hoover, **c** Slats-Frosty, **d** Slats-Wallbanger, **e** Igor and **f** Olympic prospects. NB: paragenetic stages apply only to a specific area, e.g. Slab stage 3 ≠ Hoover stage 3 ≠ Igor stage 3

edge of the Richardson Fault array (Fig. 1). This is a series of deep-seated, long-lived structures that developed in a dilational tectonic regime and are traceable for approximately 600 km in an area that marks the transition from relatively undeformed rocks of the Northern Interior Platform to those of the Cordilleran Orogenic System (Delaney 1981; Norris 1997; Thorkelson 2000).

Local scale

Breccia emplacement appears to have exploited pre-existing crustal weaknesses (cf. Bell 1986a, b; Thorkelson 2000) at all scales including the faulted cores of folds, high strain zones, pathways previously used by the BPRI, jointing/fractures and permeable sedimentary layers. Breccia occurs throughout the WSG but is most widespread in the upper FLG (Delaney 1981).

The Slab prospect is underlain by upper FLG strata (Bell and Delaney 1977) that are, in part, made up of metaevaporites (Fig. 5; Table 3). It occurs on the eastern limb of a large northwest-trending anticlinal structure proximal to a flexure in the trend of the fold (Fig. 2) and is cut by a northwest-trending zone of schist and phyllite interpreted to a be a high strain zone (Fig. 7; Thorkelson 2000; Brideau et al. 2002). Minor outcrops of BPRI occur within the strain zone. Extensive Wernecke Breccia occurs as large, elongate, irregular-shaped bodies proximal to the high strain zone, as elliptical pipe-like bodies a few metres in diameter within the strain zone and as narrow bodies parallel to layering in metasedimentary rocks. Cross-cutting relationships indicate there are at least three phases of breccia (Hunt et al. 2002). Breccias in this area contain the largest clasts observed with some up to several hundred metres across and it is one of few locations where breccia contains clasts of Slab volcanics (Fig. 7; cf. Thorkelson 2000; Hunt et al. 2002; Laughton et al. 2002; Laughton 2004). A detailed description of part of the Slab area (Slab creek) is given in Brooks et al. (2002) and Brooks (2002).

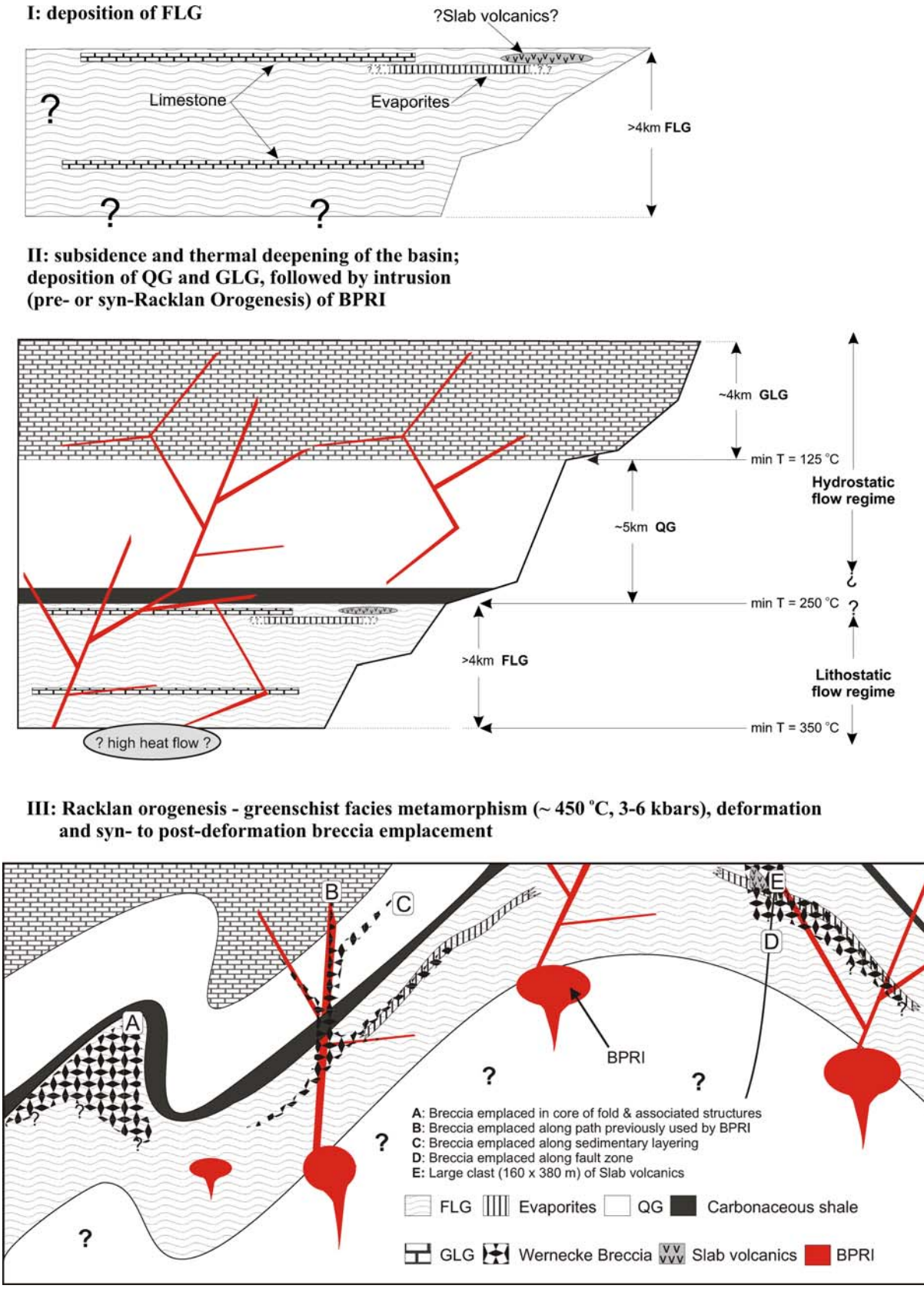

Fig. 14 Cartoon depicting evolution of Wernecke Basin and structural controls on location of Wernecke Breccia. Stage I: deposition of FLG. Stage II: deposition of Quartet group and GLG. Stage III: emplacement of Wernecke Breccia into pre-existing weak zones in deformed and metamorphosed WSG. Breccia bodies are widespread at the top of FLG in metaevaporite-bearing stratigraphy. See text for detailed description of stages

The Hoover prospect is located about 20 km north of Slab and is underlain dominantly by FLG to Quartet Group transitional rocks including a 4–10 m-thick regional marker carbonate unit (Figs. 2, 8; Thorkelson et al. 2002, 2003). Like Slab, Hoover occurs on the eastern limb of the antiform whose axis underlies the Bonnet Plume River valley (*ibid.*). Wernecke Breccia occurs in two locations (Fig. 8; *ibid.*): (1) an irregular-shaped breccia body at least 100 m thick occurs at the base of the slope in strongly folded FLG metasiltstone and phyllite and (2) small, discontinuous breccia bodies 1–20 m thick occur about 500 m upslope in Quartet Group at the contact between slate and metasiltstone. Large (up to 12×10 m) clasts of BPRI diorite are abundant locally in the lower breccia. Rare clasts of earlier breccia indicate that there have been multiple episodes of brecciation.

The Igor prospect, located about 28 km west of Slab, is underlain by Quartet Group metasedimentary rocks (unit Q-2 of Delaney 1981) that are faulted against and unconformably overlain by Paleozoic clastic sedimentary rocks and limestone (Figs. 2, 9; cf. Norris 1997). Quartet Group rocks have been folded into a north-trending anticline. The core of the anticline is coincident with schistose rocks that probably represent a high strain zone. Abundant Wernecke Breccia occurs in the core of the anticline and cross-cutting relationships indicate several phases of breccia are present. In addition, narrow zones of breccia ($<$ 2 m wide) occur in Quartet Group adjacent to the main breccia complex.

Slats-Frosty is located about 15 km west of Slab and is underlain by the FLG and abundant BPRI dykes and sills (Fig. 2; Thorkelson et al. 2002, 2003). It is located on the east side of a large northeast-trending overturned antiform (Thorkelson 2000; Thorkelson et al. 2002, 2003). Breccia occurs dominantly as numerous discontinuous narrow bands up to 1.5 m thick emplaced parallel to layering in the FLG, and less commonly as narrow zones (up to 0.8 m) parallel to prominent jointing. The Slats-Wallbanger prospect is located approximately 4 km south of Slats-Frosty and is underlain by Quartet Group-GLG transitional strata (units Q-2 and G-Tr of Delaney 1981) and abundant BPRI (Thorkelson 2000). Breccia occurs throughout the Wallbanger area as narrow bands (2 m across) and larger irregular bodies proximal to BPRI rocks. The Olympic prospect, located approximately 15 km southeast of Slab, occurs in the upper part of the WSG and is underlain by GLG dolostone and BPRI (Fig. 2; *cf.* Thorkelson 2000). The dolostone is in part stromatolitic (Fig. 4e, unit G-5 or G-7 of Delaney 1981) and intra-formational dolostone breccia is locally abundant. Wernecke Breccia occurs as irregular-shaped bodies in the Olympic area that locally contain abundant clasts of BPRI anorthosite, from $<$ 1 cm to tens of metres across (Thorkelson 2000; this study). Sparse clasts of earlier breccia indicate multiple phases of brecciation have occurred.

Alteration

Extensive metasomatic alteration occurs within Wernecke Breccia and extends into host WSG and/or BPRI rocks for a few metres to tens of metres (cf. Thorkelson 2000, Hunt et al. 2002, 2003a, b). There are two major alteration types, sodic and potassic whose abundance appears to depend on host rock lithology. Sodic alteration generally occurs in breccia hosted by lower WSG rocks where there is evidence for metaevaporites. Breccia and WSG rocks affected by sodic alteration are dominantly grey in colour (Fig. 10a) and contain abundant albite and lesser scapolite. This type of alteration is dominant, for example, at Slab and Hoover where feldspar from breccia clasts, breccia matrix, veins and sedimentary rocks is dominantly albite (Fig. 11a); feldspar at Slab is composed of $albite_{96\text{-}100}$, $orthoclase_{0\text{-}1}$and $anorthite_{0\text{-}4}$ and at Hoover is composed of $albite_{98\text{-}100}$, $orthoclase_{0\text{-}1}$ and $anorthite_{0\text{-}2}$. Minor orthoclase occurs in both areas (Fig. 11a) and has a narrow compositional range of $orthoclase_{86\text{-}99}$, $albite_{0\text{-}16}$, and $anorthite_{0\text{-}14}$.

Potassic alteration is dominant in breccias hosted by fine-grained clastic rocks i.e. in the Quartet Group, in the FLG where no evidence for metaevaporites was observed, and in the GLG where dolostone is interlayered with fine-grained clastic rocks. Rocks affected by potassic alteration are largely pink to red in colour and contain abundant orthoclase $\pm$ sericite (Fig. 10b). This type of alteration occurs, for example, at Slats-Frosty and Olympic where feldspar is dominantly orthoclase (Fig. 11a); feldspar at Slats-Frosty is composed of $orthoclase_{94\text{-}99}$, $albite_{0\text{-}6}$, $anorthite_{0\text{-}1}$ and at Olympic is composed of $orthoclase_{88\text{-}100}$, $albite_{0\text{-}9}$, $anorthite_{0\text{-}6}$. Metasomatic alteration at Igor is dominantly potassic consisting of orthoclase and sericite; minor albite is present (Fig. 11a). Feldspar at Igor is composed of $orthoclase_{82\text{-}96}$, $albite_{3\text{-}18}$, $anorthite_{0\text{-}1}$and $albite_{99\text{-}100}$, $orthoclase_{0\text{-}1}$, $anorthite_{0\text{-}1}$.

At all of the prospects examined, sodic or potassic alteration is overprinted by carbonate that forms the dominant phase in breccia matrix and cross-cutting veins (Fig. 10c, d). The composition of the carbonate also varies. Calcite is dominant in breccias with sodic alteration, for example at Slab and Hoover (Fig. 11b); dolomite occurs in minor amounts. Dolomite and ankerite are dominant in potassically-altered breccias, for example at Slats-Frosty and Olympic. The Igor prospect differs from others in the study in that siderite, in addition to dolomite/ankerite, is locally abundant in breccia matrix and narrow cross-cutting veins (Fig. 11b). Igor is also the only prospect studied where barite is abundant. It occurs as veins, lenses or pods (locally coarsely crystalline) up to 3 m×15 m that cross-cut breccia, and as disseminations within breccia matrix and zones of massive magnetite-hematite (Archer 1980; Eaton and Archer 1981; this study).

Mineralization

Sixty-five Wernecke Breccia-associated prospects are known from the Wernecke and Ogilvie Mountains and all are associated with IOCG mineralization (Fig. 1, Archer and Schmidt 1978; Yukon MINFILE 2003). Mineralization is similar at each prospect and occurs as veins and disseminations in breccia and surrounding rocks and locally as breccia matrix; multiple episodes of mineralization are evident (Figs. 1, 10, 12; cf. Archer and Schmidt 1978; Yukon MINFILE 2003; Hunt et al. 2002, 2003a; Brooks et al. 2002). IOCG minerals include magnetite, hematite, chalcopyrite and lesser pitchblende, brannerite and cobaltite; gold was not observed but reports with copper in assay results (cf. Archer and Schmidt 1978; Yukon MINFILE 2003; Brooks 2002). General descriptions of mineralization at the prospects studied are given below. The characteristics of each prospect, including main mineral assemblage and resource or best intersection, are summarized in Table 3.

Multiple phases of oxide and sulphide mineralization occur at Slab which has a resource of 20 mt of 0.35% Cu and 0.17 g/t Au (Thorkelson et al. 2003). Magnetite is dominant in the early stages of brecciation and locally occurs as massive ankerite–magnetite veins up to 1 m across (Fig. 10e; Hunt et al. 2002). These are cross-cut by and occur as clasts in later breccia. Lesser amounts of magnetite occur in later paragenetic stages as disseminated fine-grained blebs and euhedral crystals. Hematite, chalcopyrite and pyrite occur throughout the paragenesis but are most abundant during brecciation following ankerite-magnetite alteration when they occur mainly as breccia matrix and syn-breccia veins (Figs. 10f). Breccia locally contains clasts of massive pyrite–chalcopyrite up to 20 cm across indicating multiple phases of sulphide mineralization (Fig. 10g). All breccia is cut by veins up to 1 m thick composed dominantly of calcite ± quartz-albite–hematite–magnetite–muscovite–biotite–fluorite. These veins locally contain chalcopyrite (Fig. 10h) and pyrite and rarely molybdenite.

Breccia-associated mineralization at Hoover is similar to that at Slab and occurs along the northeast side of the Bonnet Plume River valley for over 6 km (Fig. 2); best intersections returned 0.32 g/t Au and 0.42% Cu over 73 m and 3.6% Cu over 3.1 m (Thorkelson et al. 2003; Yukon MINFILE 2003). Mineralization is dominantly copper–gold with minor uranium and cobalt and occurs: (1) as disseminations in albite-quartz-pyrite-chalcopyrite veinlets/replacement layers within siltstone clasts in the breccia and as rare massive sulphide clasts, (2) as disseminations and blebs in breccia matrix, locally forming the entire matrix (Fig. 10i), 3) as blebs up to 5 cm across and disseminations in calcite-chlorite-muscovite-pyrite-chalcopyrite-hematite ± magnetite, quartz–hematite–pyrite–chalcopyrite and calcite ± chalcopyrite veins that cross-cut breccia and WSG and (4) as blebs and disseminations in quartz-chalcopyrite ± feldspar ± muscovite ± hematite veins that are parallel to and cross-cut calcareous layers in siltstone. In general, mineralization occurs as large zones of low-grade copper–gold that contain higher grade pockets (Table 3).

At the Igor prospect, mineralization occurs largely as pods up to 4×15 m of massive hematite–magnetite–pyrite–chalcopyrite and minor pitchblende with dolomite, ankerite, siderite, barite, quartz and chlorite (Archer 1976, 1980; Eaton and Archer 1981; Eaton 1982; this study). The pods occur within breccia in east-trending fractures that are approximately orthogonal to the axis of the large anticline in Igor creek, and in narrow bands parallel to foliation in breccia. Within the pods, hematite, pyrite and/or chalcopyrite locally form/?replace breccia matrix. Less abundant mineralization occurs as disseminations in breccia and Quartet group rocks and in quartz ± siderite ± chalcopyrite ± hematite ± pyrite ± magnetite veins, barite veins and dolomite veins that cut the massive mineralization. Drilling produced encouraging results including a 19.7 m intersection of 4.74% Cu, 0.088% U_3O_8 and 325 ppm Co and a separate 10.6 m intersection of 6.14% Cu, 0.89% U_3O_8 and 358 ppm Co (Eaton and Archer 1981). Cobalt is associated with pyrite and is unevenly distributed between pyrite grains (Eaton and Archer 1981). In some instances, a cobalt-bearing pyrite grain is surrounded by barren pyrite grains. Uranium mineralization appears to be related to chalcopyrite and occurs mainly as pitchblende: (1) associated with barite and minor chalcopyrite that discontinuously fills fractures/joints in breccia, (2) as disseminations in zones of chalcopyrite-rich massive magnetite-hematite and (3) as rims on breccia clasts and disseminations in breccia matrix (Archer 1980). Thorium is a minor constituent; U:Th is 47:1. Uranium is also found in rare brannerite that occurs in fractures in metasedimentary rocks adjacent to breccia (Eaton and Archer 1981).

At the Slats prospects (Frosty and Wallbanger) copper ± gold ± cobalt mineralization is widely distributed and low grade with sporadic higher grade occurrences (Table 3). In general, at Frosty, chalcopyrite occurs as disseminations in breccia and in veins and fractures. Pods/veins of massive hematite or massive magnetite-coarsely crystalline hematite-ankerite-quartz up to 2×4 m^2 occur locally in breccia zones (Fig. 12a); samples returned low values of copper and gold with the best results (1,380 ppb Au and 9,650 ppm Cu) being returned by a grab sample (Thorkelson et al. 2003). Quartz vein material containing visible gold and brannerite also occurs in the Frosty area (Yukon MINFILE 2003). Selected samples returned values of 686 to 10,285 g/t Au (*ibid*), however the source of this material has not been found and it is not known if it is related to Wernecke Breccia. Mineralization at Wallbanger is similar to that in other areas (Table 3); pyrite locally forms the breccia matrix and a pod of massive magnetite occurs at a contact between breccia and shale; the best intersection returned 450 ppb Au, 1,115 ppm Cu and 5,800 Co over 1 m (Stammers 1995). IOCG mineralization at the

Olympic prospect is generally low grade and not abundant; the best intersection returned 1,593 ppm Cu, 40 ppm Co and 23 ppb Au over 11 m (Table 3; Caulfield 1994). The observed mineralization consists of chalcopyrite and pyrite on fractures at siltstone-breccia contacts, euhedral pyrite + chalcopyrite ± erythrite in ankerite–quartz veins in crackle brecciated siltstone, and sparse chalcopyrite porphyroblasts that overprint breccia matrix and clasts.

Paragenesis

Broad paragenetic sequences were established for the breccia occurrences based on cross-cutting relationships in outcrop and drill core (Fig. 13; Hunt et al. 2002, 2004). Paragenetic stages are unique to each prospect and not equivalent to those of other areas; for example Slab stage 3 ≠ Hoover stage 3 ≠ Olympic stage 3. Each phase in the development of a breccia complex was probably multi-stage and overlapped other stages (Delaney 1981). However, there is an overall general trend of: (1) metasomatic alteration (sodic or potassic) that overprints greenschist facies metamorphic mineral assemblages; (2) early stage brecciation accompanied by abundant magnetite ± hematite alteration; (3) main phase of brecciation accompanied by hematite and chalcopyrite–pyrite ± magnetite mineralization; and (4) syn to post breccia carbonitization (calcite, ankerite/dolomite, siderite) ± pyrite, chalcopyrite, hematite, magnetite. Locally barite veins are abundant during stage 4 (e.g. at Igor). During the main phase of brecciation early euhedral magnetite is commonly replaced by hematite (Fig 12b) and/or pyrite (Fig. 12c) and, in general, where chalcopyrite is present with other metallic minerals it is usually the latest mineralization phase (Fig. 12d).

Discussion

Timing of breccia emplacement

Cross-cutting relationships demonstrate Wernecke Breccia was emplaced syn- to post-Racklan orogenesis, after peak metamorphism. Sodic and potassic metasomatic alteration associated with Wernecke Breccia overprints greenschist facies metamorphic assemblages and all breccia bodies examined contain clasts of foliated metasedimentary rocks (Fig. 12e) thus indicating that Wernecke Breccia was emplaced after commencement of Racklan orogenesis. Syn-deformation breccia emplacement is indicated by foliated breccia at the Igor prospect that occurs as clasts within cross-cutting breccia that does not contain a fabric (Eaton and Archer 1981) and by kinked breccia-related ankerite-magnetite and magnetite veins at Slab (Fig. 12f). Post-deformation breccia emplacement is demonstrated by the presence of phyllite clasts in the breccia that contain all three phases of deformation, e.g. Slab (Thorkelson 2000). Locally, Wernecke Breccia contains clasts of foliated metasiltstone and is itself foliated (Fig. 12g), e.g. at Slats-Wallbanger, however, it is not clear if this deformation is related to Racklan orogenesis or to later deformation.

The absolute age of Wernecke Breccia is constrained by a U–Pb age of ca. 1,600 Ma that was returned by hydrothermal titanite from a sample of breccia matrix at Slab (Thorkelson 2000; Thorkelson et al. 2001a); this breccia contains foliated, crenulated, kinked clasts of WSG rocks (*ibid*). Additional age dating is being carried out as part of this project and samples have been submitted for Ar–Ar, Re–Os and U–Pb analysis (Hunt 2005).

Mechanism of breccia emplacement

Several hypotheses have been suggested for the mechanism of breccia emplacement including mud diapirs (Lane 1990), phreatomagmatic explosions (Laznicka and Edwards 1979), diatremes (Tempelman-Kluit 1981; Bell and Delaney 1977), modified evaporite diapirs (Bell 1989) and explosive expansion of volatile-rich fluids associated with deeply buried intrusions (Thorkelson 2000; Thorkelson et al. 2001a). Recent studies place constraints on these possible mechanisms (cf. Thorkelson 2000 for a review). For example: (1) mud diapirism is ruled out because Wernecke Breccia contains clasts of deformed WSG rocks indicating that the sediments were lithified and deformed prior to brecciation; (2) a diatreme origin seems unlikely because breccia clasts are locally derived; (3) age dating shows that breccia is considerably younger than BPRI (ca. 1600 versus ca. 1710 Ma) making BPRI magmatism an unlikely mechanism of brecciation; and (4) brecciation caused by the explosive expansion of volatile-rich fluids derived from deeply buried intrusive rocks appears unlikely because stable isotope data do not indicate input from magmatic fluids (see below; Hunt et al. 2004, and in preparation).

Any model for the formation of Wernecke Breccia must take into account the following observations: (1) the large-scale of the brecciation and metasomatic alteration; (2) multiple phases of cross-cutting breccia and mineralization; (3) the spatial association of breccia with regional-scale faults and the occurrence of breccia bodies in weak zones such as cores of folds and faults; (4) the spatial association of breccia with BPRI and the age difference between breccia and BPRI; (5) the emplacement of breccia syn- to post-Racklan deformation and after peak metamorphism; (6) the widespread occurrence of breccia in the upper FLG; (7) the presence of metaevaporites in the upper FLG; (8) the preservation of Slab volcanics as clasts in breccia emplaced into the FLG; (9) the derivation of breccia clasts from proximal host rocks; and (10) the distribution of sodic and potassic metasomatic alteration.

Any proposed brecciation mechanism must also take into account characteristics of the breccia-forming fluid. Information available to date is provided by fluid

inclusion and stable isotope data (Hunt et al., 2004, and in preparation) and is summarized here: Syn-breccia fluids were low to moderate temperature (185 – 350°C), high salinity (24–42 wt. % NaCl eq.) NaCl–$CaCl_2$–H_2O brines. Carbon, oxygen and sulphur isotope results for each of the IOCG prospects studied are similar and, in general, do not vary systematically with paragenetic stage: $\delta^{13}C \sim -7$ to $+1‰$ (PDB), $\delta^{18}O \sim 9$ to $20‰$ (SMOW), $\delta^{34}S_{sulphide} \sim -12$ to $+13‰$ (CDT) and $\delta^{34}S_{sulphate} \sim 8$ to $17‰$ (CDT). The fluid composition and isotopic ratios appear to be rock buffered (*ibid*). The $\delta^{13}C$ values of hydrothermal carbonates indicate the carbon was derived in large part from the host WSG. The $\delta^{34}S$ values of hydrothermal pyrite, chalcopyrite and barite point to a seawater (or sediments/evaporites deposited from seawater) source for sulphur. These data combined with limited deuterium isotope data (in progress) indicate the source of fluids was likely formation/metamorphic water mixed with variable amounts of organic water ± evolved meteoric and/or evolved seawater (*ibid.*). Fluid inclusion data also enable the depth of breccia emplacement to be estimated. This was calculated for Slab to be 7.4 to 9.0 km (2.4–3.0 kbar; *ibid.*), thus indicating that breccia at Slab was emplaced at considerable depth and not close to surface as previously suggested (cf. Thorkelson et al. 2001a; Laughton 2004).

The following proposed brecciation mechanism takes into account the above constraints and relates breccia emplacement to evolution of the Wernecke Basin, as shown in Fig. 14.

Stage I Deposition of the lower WSG in a region underlain by attenuated continental crust (Thorkelson 2000). This is represented by the FLG calcareous sedimentary rocks and minor limestone that make up the first WSG clastic to carbonate grand cycle (Delaney 1981; Thorkelson 2000). Evaporites (halite facies) were deposited in (at least) the upper part of the FLG. Slab volcanics may also have been deposited at this time.

Stage II Subsidence and thermal deepening of the basin due to rifting, and the subsequent deposition of the middle and upper parts of the WSG (Thorkelson 2000). The transition is marked by an abrupt change from dolostone to carbonaceous shale at the top of the FLG (Delaney 1981). Quartet Group fine-grained clastic rocks and the overlying GLG dolostone were deposited at this time and form a second clastic to carbonate grand cycle (Delaney 1981; Thorkelson 2000). The accumulation of thick shallow-water carbonates in the upper part of the WSG indicates protracted subsidence of the basin during this time; abrupt facies changes within the GLG indicate normal faulting was coincident with deposition (Thorkelson 2000). The suite of BPRI were emplaced ca. 1,710 Ma, after deposition of the WSG. However, their timing with respect to deformation is poorly constrained and they could be pre- or syn-Racklan orogenesis (Thorkelson 2000; Thorkelson et al. 2001b).

Stage III Racklan Orogenesis caused greenschist facies metamorphism and three phases of deformation in WSG rocks (Thorkelson 2000; Brideau et al. 2002). Peak metamorphic conditions (450–550°C and 3–6 kbar), folds and foliations were produced during the first phase. The second and third phases produced crenulations/crenulation cleavage and kink bands respectively (*ibid.*). Cross-cutting relationships indicate that Wernecke Breccias were produced syn- to post-deformation, but post-peak metamorphism. The length of time occupied by Racklan orogenesis is poorly constrained. If the ca. 1,710 Ma. BPRI were emplaced before orogenesis then deformation and breccia emplacement could have occurred over a geologically short period of time prior to (close to) ca.1,600 Ma, the age of post-deformation breccia emplacement. However, if BPRI were emplaced syn-orogenesis this implies a period of deformation and breccia production that spanned over 100 Ma years (i.e. ca. 1,710–1,600 Ma).

During stages I and II, as the WSG sediments were undergoing diagenesis and compaction, evaporites within the sedimentary pile would have begun to dissolve. Dissolution would have caused disruption of intercalated and overlying sediments and led to the formation of solution breccias (Fig. 5), and strata overlying evaporites would have been extensively tilted and faulted (cf. Warren 1999). Temperatures would have become elevated in deeper parts of the basin due to the increasing weight of overlying sediments as deposition continued. For example, assuming a geothermal gradient of 25°C/km (average geothermal gradient of the earth, cf. Raymond 1995) and a surface temperature of 25°C, the temperature at the top of the FLG (~9 km depth) would have been 250°C (Fig. 14). Greenschist facies metamorphism with temperatures of at least 450°C was superimposed on the above scenario along with contractional deformation (Brideau et al. 2002). Wernecke Breccia was therefore produced within WSG rocks that had already been affected by syn-depositional faulting, probably contained zones of disrupted and brecciated strata associated with evaporites, had been intruded by BPRI, had reached elevated temperatures due to burial and metamorphism and had been affected by at least one phase of deformation.

The brecciation mechanism that produced Wernecke Breccia was probably not violently explosive, i.e. not diatreme- or volcanic-like. Clasts are derived from proximal host strata and do not show evidence of transport. Clasts of country rocks are commonly angular to subangular and locally, have clear jigsaw-fit texture (e.g. Fig. 10i); this is especially apparent where breccia cross-cuts BPRI or well-laminated sedimentary rocks. Subrounded to rounded clasts (e.g. Figs. 6c, 10a) and intense zones of alteration also occur, generally in areas where cross-cutting relationships demonstrate that multiple brecciation events have occurred. The amount of fluid was probably not voluminous, as evidenced by the rock buffered nature of alteration and isotopic

ratios, except in areas of cross-cutting breccia which likely mark zones of more abundant fluid flow.

This evidence best fits a scenario in which breccias were created by the relatively non-violent expansion of over-pressured basinal fluids. These fluids were locally focussed along permeable pathways, such as faults or shear zones, which led to multiple brecciation events in the same location as pressure repeatedly built up and was released. Basinal fluid would likely have become over-pressured during burial and compaction of sediments, especially in deeper parts of the basin where plastic deformation would be likely to decrease permeability and close porosity leading to an increase in pore fluid pressure (McCaig et al. 2000). It is probable that pressure within basinal fluids would have been released during initial phases of Racklan deformation. However, in situ evaporites were still present during metamorphism and could have acted as a local seal to fluid flow. In addition, at least at Slab, breccia was emplaced at considerable depth (7–9 km) and strata may have been deforming plastically which would cause over-pressuring of the pore fluid if no permeable pathways such as faults were available. Periodic release of pressure, perhaps by breaking of seals on permeable pathways during continuing deformation, would lead to rapid expansion of fluid and the formation of breccia, particularly in weak, fractured zones such as the cores of folds. In order to maintain repeated brecciation events fluid would have to be added to the system. This may explain why Wernecke Breccia is spatially related to the large-scale Richardson Fault array. These crustal-scale faults could have allowed fluids to enter the basin and recharge the system. The occurrence of widespread breccia bodies in upper FLG strata compared to the rest of the WSG (Delaney 1981) may be due to the presence of metaevaporites in this part of the stratigraphy. Dissolution of evaporites during diagenesis, compaction and metamorphism would have caused disruption of intercalated and overlying sediments and led to the formation of solution breccias (Warren 1999) thus providing widespread weak zones that could be utilized by over pressured fluids to produce brecciation. Wernecke Breccias that occur at this stratigraphic level contain the largest clasts observed (hundreds of metres across) and this also may be related to the presence of evaporites. Large blocks could initially have been formed during evaporite dissolution due to foundering of strata overlying evaporite layers. These blocks could then have become entrained in Wernecke Breccia as fluid utilized the pre-existing weak, and probably permeable zone during breccia emplacement.

Summary

In summary, zones of Wernecke Breccia occur over a large part of north-central Yukon in areas of regional-scale faulting. They occur throughout host WSG strata but are most widespread in lower WSG where metaevaporites make up part of the stratigraphy. WSG strata and breccia proximal to metaevaporites have been affected by dominantly sodic metasomatism. WSG rocks and breccias distal to evaporites have undergone mainly potassic metasomatism. Sodic and potassic alteration are overprinted by carbonate alteration. IOCG mineralization is associated with the breccia bodies and occurs as disseminations, veins and breccia matrix. Cross-cutting relationships indicate multiple alteration, brecciation and mineralizing events. Breccia emplacement occurred in weak zones of the crust and was probably caused by the expansion of over pressured basinal fluids. Fluids that formed the breccias were low to moderate temperature, high salinity $NaCl–CaCl_2–H_2O$ brines probably derived from dominantly basinal sources. There is no evidence for the input of magmatic fluids and the high salinity of the fluid is interpreted to be due to interaction with (halite facies) evaporites (Hunt et al.2004; in preparation). Thus, the fluids involved are similar to those proposed by Barton and Johnson (1996, 2000) for the formation of some IOCG deposits.

Wernecke Breccias were emplaced into a thick, dominantly marine sedimentary sequence that was likely deposited in an intra-continental rift basin setting (cf. Thorkelson 2000). Other IOCG districts that formed in a similar tectonic environment and also have large-scale brecciation and metasomatic alteration include those of the Cloncurry district in Australia and the Lufilian arc in central Africa (Hitzman 2000). Little is known about the IOCG mineralization in central Africa however, the Cloncurry district, has received much exploration attention and several deposits have been discovered including the large Ernest Henry (167 Mt at 1.1% Cu, 0.54 g/t Au) deposit (cf. Ryan 1998; Williams and Skirrow 2000; Mark et al. 2000). Breccia-associated IOCG prospects in the Wernecke Mountains contain evidence for multiple cross-cutting brecciation and mineralizing events (cf. Yukon MINFILE 2003) but they have received little exploration to date and their full potential remains unknown.

Acknowledgements Funding for this project is provided by the Yukon Geological Survey, an Australian International Postgraduate Research Scholarship, a James Cook University scholarship and Merit Research Grant, a Society of Economic Geologists Student Research Grant, and a predictive mineral discovery* Cooperative Research Centre scholarship. Newmont Mining Corporation, Archer, Cathro and Associates (1981) Ltd, Equity Engineering, Pamicon Developments, Monster Copper Resources and Blackstone Resources kindly provided access to confidential data, drill core and/or properties. The manuscript benefited from helpful reviews by Dan Kontak and Mark Barton and from editorial comments by Iain McDonald.

References

Archer AR (1976) Report on soil geochemistry, geology and radiometric survey Igor 1–26 claims. Yukon Assessment Report 090083, 8 pp

Archer AR (1980) Drill report Igor 1–26 claims. Yukon Assessment Report 090562, 12 pp
Archer AR, Schmidt U (1978) Mineralised breccias of early Proterozoic age, Bonnet Plume River District, Yukon Territory. CIM Bulletin 71:53–58
Archer A, Bell RT, Delaney GD, Godwin CI (1977) Mineralized breccias of Wernecke Mountains Yukon. Geological Association of Canada Program with Abstracts 2:5
Barton MD, Johnson DA (2000) Alternative brine sources for Fe-oxide(–Cu–Au) systems: implications for hydrothermal alteration and metals. In: Porter TM (ed) Hydrothermal Iron oxide copper-gold and related deposits: a global perspective, vol. 1. PGC Publishing, Adelaide, pp 43–60
Barton MD, Johnson DA (1996) Evaporitic-source model for igneous-related Fe oxide-(REE-Cu-Au-U) mineralization. Geology 24(3):259–262
Bell RT (1989) A conceptual model for development of megabreccias and associated mineral deposits in Wernecke Mountains, Canada, Copperbelt, Zaire, and Flinders Range, Australia. In: Uranium resources and geology of North America: proceedings of a technical committee meeting, organized by the Internal Atomic Energy Agency held in Saskatoon, Canada, 1987, pp 149–169
Bell RT (1986a) Megabreccias in northeastern Wernecke Mountains, Yukon Territory. Current Research, Part A, Geological Survey of Canada, Paper 86–1A, pp 375–384
Bell RT (1986b) Geological map of north-eastern Wernecke Mountains, Yukon Territory. Geological Survey of Canada, Open File 1027
Bell RT (1978) Breccias and uranium mineralization in the Wernecke Mountains, Yukon Territory – a progress report. Current Research, Part A, Geological Survey of Canada, Paper 78–1A, pp 317–322
Bell RT, Delaney GD (1977) Geology of some uranium occurrences in Yukon Territory. Report of Activities, Part A, Geological Survey of Canada, Paper 77–1A, pp 33–37
Brideau M-A, Thorkelson DJ, Godin L, Laughton JR (2002) Paleoproterozoic deformation of the Racklan Orogeny, Slats Creek (106D/16) and Fairchild Lake (106C/13) map areas, Wernecke Mountains, Yukon. In: Emond DS, Weston LH, Lewis LL (eds) Yukon exploration and geology 2001, exploration and geological services division, Yukon Region, Indian and Northern Affairs Canada, pp 65–72 (This items can be downloaded from the Yukon Geological Survey website http://www.geology.gov.yk.ca)
Brooks M (2002) Alteration, brecciation and Fe oxide-Cu (-Au) mineralisation at Slab creek, Yukon Territory, Canada. Honours Thesis, James Cook University, 113 pp
Brooks M, Baker T, Hunt J (2002) Alteration zonation, veining and mineralization associated with the Wernecke Breccias at Slab creek, Yukon Territory, Canada. In: Emond DS, Weston LH, Lewis LL (eds) Yukon exploration and geology 2001, exploration and geological services division, Yukon Region, Indian and Northern Affairs Canada, pp 249–258 (This items can be downloaded from the Yukon Geological Survey website http://www.geology.gov.yk.ca)
Caulfield DA (1994) Olympic property diamond drilling logs. Yukon Assessment Report 093222, 40 pp
Deer WA, Howie RA, Zussman J (1992) An introduction to rock forming minerals, 2nd edn. Longman Scientific & Technical, 696 pp
Delaney GD (1978) A progress report on stratigraphic investigations of the lowermost succession of Proterozoic rocks, northern Wernecke Mountains, Yukon Territory. Exploration and Geological Services Division, Yukon Region, Indian and Northern Affairs Canada, Open File Report EGS 1978–10, 12 pp (This items can be downloaded from the Yukon Geological Survey website http://www.geology.gov.yk.ca)
Delaney GD (1981) The Mid-Proterozoic Wernecke Supergroup, Wernecke Mountains, Yukon Territory; In: Proterozoic Basins of Canada, Geological Survey of Canada, Paper 81–10, pp 1–23
Eastoe CJ, Long A, Knauth LP (1999) Stable chlorine isotopes in the Palo Duro Basin, Texas: evidence for preservation of Permian evaporite brines. Geochim Cosmochim Acta 63:1375–1382
Eaton WD (1982) Wernecke Joint Venture diamond drill report Igor 1–26 claims. Yukon Assessment Report 091445, 17 pp
Eaton WD, Archer AR (1981) Wernecke joint venture drill report Igor 1–26 claims. Yukon Assessment Report 090756, 13pp
Gabrielse H (1967) Tectonic evolution of the northern Canadian Cordillera. Can J Earth Sci 4:271–298
Gordey SP, Makepeace AJ (1999) Yukon digital geology. Exploration and Geological Services Division, Yukon Region, Indian and Northern Affairs Canada, Open File 1999–1 (D). Also available as Geological Survey of Canada Open File D3826 (This items can be downloaded from the Yukon Geological Survey website http://www.geology.gov.yk.ca)
Hitzman MW (2000) Iron oxide–Cu–Au deposits: what, here, when, and why? In: Porter TM (ed) Hydrothermal iron oxide copper-gold and related deposits: a global perspective, vol. 1, pp 9–25
Hunt JA, Laughton JR, Brideau M-A, Thorkelson DJ, Brookes ML, Baker T (2002) New mapping around the Slab iron oxide-copper-gold occurrence, Wernecke Mountains. In: Emond DS, Weston LH, Lewis LL (eds) Yukon Exploration and Geology 2001, Exploration and Geological Services Division, Yukon Region, Indian and Northern Affairs Canada, pp 125–138 (This items can be downloaded from the Yukon Geological Survey website http://www.geology.gov.yk.ca)
Hunt JA (2005) The geology and genesis of iron oxide-copper-gold mineralisation associated with Wernecke Breccia, Yukon, Canada. PhD Thesis, James Cook University, Townsville, Australia, 120 pp
Hunt JA, Baker T, Thorkelson DJ (2003a) Basin-scale breccia processes associated with proterozoic iron oxide-copper-gold mineralisation: an example from the Wernecke Mountains, Canada. In: The Geological Society 2003 Fermor Flagship Meeting, World Class Mineral Deposits and Earth Evolution, extended abstracts. Applied Earth Science, Transactions of the Institutions of Mining and Metallurgy, Sect. B, vol. 112(2):204–206
Hunt JA, Baker T (2003b) Wernecke Breccia-associated iron oxide-Cu-Au mineralization, Yukon, Canada. In: Eliopoulos DG et al (eds) Mineral exploration and sustainable development, Proceedings of the 7th biennial SGA meeting, Athens, Greece, vol. 2, pp 985–987
Hunt JA, Baker T, Davidson G, Fallick AE, Thorkelson DJ (2004) Origin of Wernecke Breccia: results of fluid inclusion and stable isotope analyses. Abstract, GSA Convention, Hobart, Tasmania, February 2004
Kwak TAP (1977) Scapolite compositional change in metamorphic gradient and its bearing on the identification of metaevaporite sequences. Geol Mag 114:343–354
Lane RA (1990) Geologic setting and petrology of the Proterozoic Ogilvie Mountains Breccia of the Coal Creek inlier, southern Ogilvie Mountains, Yukon Territory. MSc thesis, University of British Columbia, Vancouver, Canada, 223 pp
Laughton JR (2004) The Proterozoic Slab volcanics of northern Yukon, Canada: megaclasts of a volcanic succession in Proterozoic Wernecke Breccia, and implications for the evolution of northwestern Laurentia. PhD Thesis, Simon Fraser University, Burnaby, British Columbia, Canada, 123 pp
Laughton JR, Thorkelson DJ, Brideau M-A, Hunt JA (2002) Paleoproterozoic volcanism and plutonism in the Wernecke Mountains, Yukon. In: Emond DS, Weston LH, Lewis LL (eds) Yukon exploration and geology 2001, Exploration and geological services division, Yukon Region, Indian and Northern Affairs Canada, pp 139–145 (This items can be downloaded from the Yukon Geological Survey website http://www.geology.gov.yk.ca)
Laznicka P, Edwards RJ (1979) Dolores Creek, Yukon—a disseminated copper mineralization in sodic metasomatites. Econ Geol 74:1352–1370

Mark G, Oliver NHS, Williams PJ, Valenta RK, Crookes RA (2000) The evolution of the Ernest Henry Fe-oxide–(Cu–Au) hydrothermal system. In: Porter TM (ed) Hydrothermal iron oxide copper-gold & related deposits: a global perspective, vol. 1, pp 123–136

McCaig AM, Tritlla J, Banks DA (2000) Fluid mixing and recycling during Pyrenean thrusting: evidence from fluid inclusion halogen ratios. Geochimi Cosmochimi Acta 64(19):3395–3412

Norris DK (1997) Geology and mineral and hydrocarbon potential of northern Yukon Territory and northwestern district of Mackenzie. Geological Survey of Canada, Bulletin 422, 401 pp

Raymond J (1995) Petrology: The study of igneous, metamorphic and sedimentary rocks. McGraw-Hill Higher Education, New York, 742 pp

Reynolds LJ (2000) Geology of the Olympic Dam Cu–U–Au–Ag–REE deposit. In: Porter TM (ed) Hydrothermal iron oxide-copper-gold & related deposits: a global perspective, vol. 1, PGC Publishing, Adelaide, pp 93–104

Ryan (1998) Ernest Henry copper-gold deposit. In: Australasian Institute of Mining and Metallurgy Monograph 22, pp 759–768

Sillitoe RH (2003) Iron oxide copper-gold deposits: an Andean view. Mineral Deposit 38:787–812

Stammers MA (1995) 1995 drilling report on the Slats mineral claims. Yukon Assessment Report 093436, 19 pp

Tempelman-Kluit DJ (1981) Nor, summary of assessment work and description of mineral properties. In: Yukon Geology and Exploration, 1979–1980, Exploration and Geological Services Division, Yukon, Indian and Northern Affairs Canada, pp 300–301 (This items can be downloaded from the Yukon Geological Survey website http://www.geology.gov.yk.ca)

Thorkelson DJ (2000) Geology and mineral occurrences of the Slats Creek, Fairchild Lake and ''Dolores Creek'' areas, Wernecke Mountains, Yukon Territory. Exploration and Geological Services Division, Yukon Region, Indian and Northern Affairs Canada, Bulletin 10, 73pp (This items can be downloaded from the Yukon Geological Survey website http://www.geology.gov.yk.ca)

Thorkelson DJ, Laughton JR, Hunt JA, Baker T (2003) Geology and mineral occurrences of the Quartet Lakes map area (NTS 106E/1), Wernecke and Mackenzie mountains, Yukon. In: Emond DS, Lewis LL (eds) Yukon Exploration and Geology 2002, Exploration and Geological Services Division, Yukon Region, Indian and Northern Affairs Canada, pp 223–239 (This items can be downloaded from the Yukon Geological Survey website http://www.geology.gov.yk.ca)

Thorkelson DJ, Laughton JR, Hunt JA (2002) Geological map of Quartet Lakes area (106E/1), Wernecke Mountains, Yukon (1:50,000 scale). Exploration and Geological Services Division, Yukon Region, Indian and Northern Affairs Canada, Geoscience map 2002–2

Thorkelson DJ, Mortensen JK, Davidson GJ, Creaser RA, Perez WA, Abbott JG (2001a) Early Mesoproterozoic intrusive breccias in Yukon, Canada: The role of hydrothermal systems in reconstructions of North America and Australia. Precamb Res 111:31–55

Thorkelson DJ, Mortensen JK, Creaser RA, Davidson GJ, Abbott JG (2001b) Early Proterozoic magmatism in Yukon, Canada: constraints on the evolution of northwestern Laurentia. Can J Earth Sci 38:1479–1494

Warren J (1999) Evaporites, their evolution and economics. Blackwell, Oxford, 438 pp

Williams PJ, Skirrow RG (2000) Overview of iron oxide-copper-gold deposits in the Curnamona Province and Cloncurry District (Eastern Mount Isa block), Australia. In: Porter TM (ed) Hydrothermal iron oxide copper-gold and related deposits: a global perspective, vol. 1, pp 105–122

Yukon MINFILE (2003) Database of Yukon mineral occurrences. Exploration and Geological Services Division, Yukon Region, Indian and Northern Affairs Canada, CD-ROM (2) (This items can be downloaded from the Yukon Geological Survey website http://www.geology.gov.yk.ca)